

APPROVED FOR RELEASE: 2007/02/08: CIA-RDP82-00850R000200050061-7

29 FEBRUARY 1980

QUANTUM ELECTRONICS²
(FOUO 3/80)

1 OF 1

FOR OFFICIAL USE ONLY

JPRS L/8959

29 February 1980

USSR Report

PHYSICS AND MATHEMATICS

(FOUO 3/80)

Quantum Electronics

FBIS

FOREIGN BROADCAST INFORMATION SERVICE

FOR OFFICIAL USE ONLY

NOTE

JPRS publications contain information primarily from foreign newspapers, periodicals and books, but also from news agency transmissions and broadcasts. Materials from foreign-language sources are translated; those from English-language sources are transcribed or reprinted, with the original phrasing and other characteristics retained.

Headlines, editorial reports, and material enclosed in brackets [] are supplied by JPRS. Processing indicators such as [Text] or [Excerpt] in the first line of each item, or following the last line of a brief, indicate how the original information was processed. Where no processing indicator is given, the information was summarized or extracted.

Unfamiliar names rendered phonetically or transliterated are enclosed in parentheses. Words or names preceded by a question mark and enclosed in parentheses were not clear in the original but have been supplied as appropriate in context. Other unattributed parenthetical notes within the body of an item originate with the source. Times within items are as given by source.

The contents of this publication in no way represent the policies, views or attitudes of the U.S. Government.

For further information on report content
call (703) 351-2938 (economic); 3468
(political, sociological, military); 2726
(life sciences); 2725 (physical sciences).

COPYRIGHT LAWS AND REGULATIONS GOVERNING OWNERSHIP OF
MATERIALS REPRODUCED HEREIN REQUIRE THAT DISSEMINATION
OF THIS PUBLICATION BE RESTRICTED FOR OFFICIAL USE ONLY.

FOR OFFICIAL USE ONLY

JPRS L/8959

29 February 1980

USSR REPORT
PHYSICS AND MATHEMATICS
(FOUO 3/80)
QUANTUM ELECTRONICS

Moscow KVANTOVAYA ELEKTRONIKA in Russian Vol 6 No 12, 1979 pp 2517-2524, 2533-2545, 2590-2596, 2606-2609, 2652-2653

CONTENTS	PAGE
Photon Branching in Chain Reactions and Chemical Lasers Initiated by Infrared Radiation (V. I. Igoshin, A. N. Orayevskiy).....	1
Prospects for Employing Porous Structures for Cooling Power Optics Components (V. V. Apollonov, et al.).....	12
Relationship Between the Statistics of Laser Damage to Solid Transparent Materials and the Statistics of Structural Defects (Yu. K. Danileyko, A. V. Sidorin).....	32
Investigation of Limiting Operating Modes of a Lamp-type Pumping Module in the 'Mikron' Laser Unit (B. V. Yerшов, et al.).....	42
Investigation of Characteristics of New Compositions for Passive Shutters for Iodine Lasers (S. P. Batashev, et al.).....	48

- a - [III - USSR - 21H S&T FOUO]

FOR OFFICIAL USE ONLY

FOR OFFICIAL USE ONLY

UDC 621.375.826

PHOTON BRANCHING IN CHAIN REACTIONS AND CHEMICAL LASERS INITIATED BY INFRA-RED RADIATION

Moscow KVANTOVAYA ELEKTRONIKA in Russian Vol 6 No 12, 1979 pp 2517-2524
manuscript received 12 Dec 78

[Article by V.I. Igoshin and A.N. Orayevskiy, USSR Academy of Sciences
Physics Institute imeni P.N. Lebedev, Moscow]

[Text] It is suggested that the molecular system $\text{CH}_3\text{F}-\text{D}_2-\text{F}_2-\text{CO}_2-\text{He}$ be employed for the purpose of creating purely chemical amplifiers of the energy of pulsed IR laser radiation. In such amplifiers laser photons take direct part in the chemical process, initiating the origin of active centers of the chain. It is demonstrated that in the system discussed it is possible for a photon-branched chain reaction to take place in which the number of photons emitted in the process of the chain's development exceeds the expenditure of photons for the purpose of creating an active center. The estimated value of the energy gain for a single amplifier stage is in the range of 10 to 1000.

If a chain reaction resulting in the induced emission of photons can be initiated by photons of the same wavelength and the emission of photons in the process of the reaction compensates or exceeds the expenditure of photons for its initiation (the formation of active centers), then the process as a whole can become self-sustained. The idea of the fundamental feasibility of such a process was expressed for the first time in [1], where the photochemical effect of IR radiation was discovered. A self-accelerating chemical reaction taking place according to this mechanism can be regarded as a reaction with a photon branching mechanism (unlike the well-known matter and energy branching in [2]). Based on reactions with photon branching it is possible to create multi-stage purely chemical laser amplifiers not requiring a supply of UV radiation energy, a discharge or an electron beam. In a cascade of amplifiers employing a photon-branched reaction, the radiation of one stage initiates a reaction in the following stage, which has greater dimensions. The possibility of amplification of the radiation energy is based on the fact that in chemical lasers employing chain reactions the fundamentally necessary expenditures of energy for initiating the reaction are much slighter than the radiation energy. Distinguished

FOR OFFICIAL USE ONLY

FOR OFFICIAL USE ONLY

especially in this respect are the systems H_2-F_2 and $D_2-F_2-CO_2$, for which the efficiency in terms of absorbed energy with initiation by an electron beam can reach approximately 1000 and 4000 to 5000 percent, respectively [3,4], with a high level of unit power output.

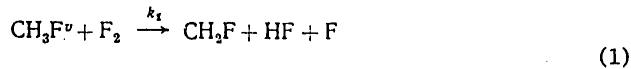
In this study is demonstrated the possibility of carrying out a reaction with photon branching and of amplifying the IR radiation in the mixture $CH_3F-D_2-F_2-CO_2-He$. In this molecular system molecules of CH_3F resonantly absorb radiation at a wavelength of 9.6 microns and then enter into a reaction with F_2 with the formation of F atoms. Here the laser chemical process is described by the following kinetic system:

The excitation of CH_3F molecules by photons with a wavelength of 9.6 microns as the result of m-fold absorption:

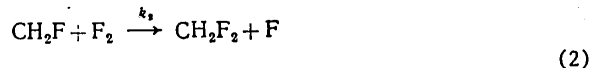


(where m is the number of photons required for activating CH_3F molecules and the symbol v designates the vibrational excitation of CH_3F).

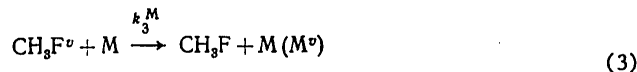
A chemical reaction between vibrationally excited molecules of CH_3F and F_2 , resulting in the formation of active centers of the chain:



A secondary reaction for the initiation of active centers:



Quenching of excited CH_3F molecules:



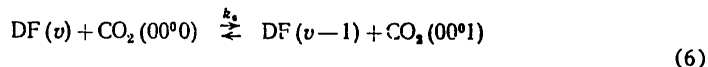
A chain reaction resulting in the formation of excited DF molecules:



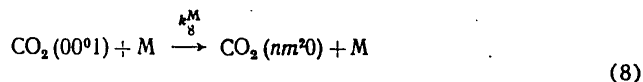
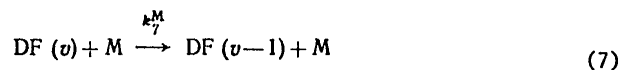
FOR OFFICIAL USE ONLY

FOR OFFICIAL USE ONLY

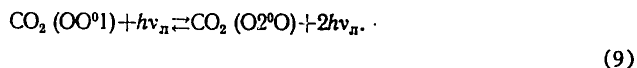
The transfer of energy from DF to CO₂:



The relaxation of excited DF and CO₂ molecules:



The coherent emission of CO₂ molecules:



Stages (0) to (3) determine the initiation of active centers under the effect of IR radiation; stages (4) to (9) are the basic stages in the operation of a chemical DF/CO₂ laser. In this system photons emerge as a full partner in the chemical process. The process described by the kinetic system presented represents a branched chain process in the case when the stages of the emission of photons and the initiation of active centers overlap in time and, in addition, the quantum yield of coherent emission, f , i.e., the number of laser photons emitted in the process of development of the chain reaction, in terms of a single active center equals

$$f > m/(\phi l),$$

where ϕ is a factor taking into account losses of vibrational quanta as the result of relaxation of CH₃F (cf. below); l is the number of active centers arising as the result of initiation reactions, equaling two in the case considered (reactions (1) and (2)).

Let us note that stages of IR initiation and radiation can be spaced over time (brief initiation as compared with the duration of the chain reaction). In addition, the frequencies of IR initiation and laser emission can be different and respond to different vibrational-rotational transitions, since the frequency of the output laser emission does not agree with the frequency responding to the effective absorption of CH₃F molecules. For example, initiation is at a wavelength of 9.6 microns and laser emission at a wavelength of 10.6 microns. This variant does not make it possible to carry out multi-stage amplification, but it can prove to be feasible for the final stage of the amplifier cascade, since in it are

FOR OFFICIAL USE ONLY

removed the restrictions caused by the presence of an absorbing medium at the lasing (amplification) frequency. Also of interest is the variant in which the initiating and output photons are emitted by different molecules. For example, initiation of the reaction by the laser emission of CO_2 molecules at a wavelength of 9.6 or 10.6 microns for the purpose of producing laser emission utilizing molecules of DF (HF) with an emission wavelength of 3.8 (2.7) microns and vice-versa. In all these variants it is better to speak not about lasers employing a reaction with photon branching, but about chemical lasers (amplifiers and generators) initiated by IR radiation. The photon-branched reaction comes under this heading as a particular case.

Up to the present time a number of experiments have been conducted on producing population inversion and lasing in vibrational-rotational transitions of HF (DF) molecules in non-chain systems $\text{SF}_6\text{-H}_2(\text{D}_2)$ [5-7], $\text{SF}_6\text{-C}_3\text{H}_8$ [7] and $\text{N}_2\text{F}_4 + \text{H}_2(\text{D}_2)$ [8,9] initiated by the emission of a CO_2 laser. In all cases studied the energy conversion factor is extremely low: 10^{-4} to 10^{-3} . With an increase in the pressure of mixtures higher than a few mm Hg, conversion efficiency drops. The addition to the working mixture of molecular fluorine for the purpose of carrying out the chain reaction does not result in a fundamental improvement of conversion efficiency [5]. The data obtained indicate the difficulty of initiating working mixtures in chemical lasers by the dissociation of SF_6 and N_2F_4 molecules under the effect of resonance irradiation by IR quanta. Here it is assumed that the formation of active centers takes place via the dissociation of irradiated molecules, which has been indicated by a number of experimental facts [10]. The low efficiency of the dissociation of molecules absorbing radiation under conditions of a laser medium is explained apparently by the rapid relaxation of excitation, which impedes the accumulation in molecules of a sufficiently great number of (a few dozen) quanta required for dissociation. It is possible that it will be possible to overcome relaxation by increasing the rate of input of energy into the system [6]. However, along this route can arise difficulties in accomplishing multi-stage amplification because of the mismatch in the duration of initiation and laser emission in the process of the chain reaction.

It is of fundamental interest to seek more effective mechanisms for the initiation of chemical lasers by employing the energy of IR radiation. In our opinion, promising for this purpose is the laser excitation of molecules with their subsequent entry into an exothermic chemical reaction accompanied by the formation of active centers. It is not possible to exclude also thermoneutral or slightly endothermic reactions. If the energy for activation of the reaction is not too high, then the necessary level of the vibrational excitation of irradiated molecules can be lowered substantially and a gain can be achieved in expenditures of energy for initiation (partly because of the exothermicity of the reaction for the initiation of centers) as compared with the case of the formation of active centers through a dissociation channel.

FOR OFFICIAL USE ONLY

FOR OFFICIAL USE ONLY

The reaction discussed in this paper, of vibrationally excited methyl fluoride with molecular fluorine resulting in the formation of F atoms, is attractive for the following reasons:

1. Molecules of methyl fluoride are able resonantly to absorb the radiation of a CO₂ laser, whereby the absorption cross section equals, according to our estimates from the data of [10,11], 10^{-19} to 10^{-18} cm² and makes possible the penetration of light to a considerable depth with CH₃F concentrations in the range of 10^{16} to 10^{17} cm⁻³ required for the formation of the required amount of atomic fluorine. Furthermore, the distributed losses remain severalfold lower than the unsaturated gain of a DF/CO₂ laser.
2. The vibrational-translational relaxation of CH₃F is a rather slow process, taking place in $1.5 \cdot 10^4$ gas kinetic collisions [12].
3. The reaction for the initiation of active centers [1] takes place, as will be estimated below, with a moderate level of vibrational excitation of CH₃F and is fast enough to enable the required speed for the production of F atoms and to compete with the relaxation of excitation through channel (3).
4. The CH₂F radical formed in the reaction of vibrationally excited methyl fluoride with fluorine quickly reacts with F₂, forming a second F atom. This reduces twofold expenditures of energy for the formation of an active center.

Let us estimate the achievable energy gain in a DF/CO₂ laser initiated by IR radiation. We will assume that activation of CH₃F molecules under the high-pressure conditions considered below takes place as the result of the successive absorption by a molecule of m quanta in a resonance transition. The higher state of a resonance absorbing transition at high pressures is rapidly devastated on account of transition of the molecule into other states, and the lower is just as quickly filled during molecular collisions, and over a wide range of intensities of IR radiation the process of activation is limited by the stage of absorption. The accumulation of energy in a molecule can be accomplished concomitantly according to another mechanism, too: It is known that polyatomic molecules are capable of effectively collecting energy in a field of IR radiation in the absence of collisions [13,14]. However this does not alter the essence of the conclusions drawn regarding the energetics of the system.

Let us analyze mathematically a simpler variant of energy conversion in which it is possible to disregard the influence of photons emitted in the process of the reaction on the process of initiation, which corresponds to the case of spaced frequencies of the initiating and emitted photons. In this variant all the energy required for initiation is supplied by the input pulse of IR radiation. It is clear that if the amplification of energy is possible in this variant, then it is all the more possible under

FOR OFFICIAL USE ONLY

conditions of a photon-branched reaction, when a not too great portion of the emitted photons goes toward initiation, making it possible, however, to lower considerably the energy requirements for the external initiating pulse. The dynamics of a photon-branched reaction are more complex and require a numerical analysis, but it is possible to expect in this case a growth in energy gain of two- to threefold as a minimum, because of the "milder" conditions of excitation.

Within the framework of the assumptions made, the kinetic equations describing the process of initiation of the chain reaction are written in the form

$$\frac{dn_{\text{CH}_3\text{F}^v}}{dt} = \frac{\sigma I}{m} n_{\text{CH}_3\text{F}} - n_{\text{CH}_3\text{F}^v} \left(k_1 n_{\text{F}} + \sum_M k_3^M n_M \right), \quad (10)$$

$$\frac{dn_a}{dt} = 2k_1 n_{\text{CH}_3\text{F}^v} n_{\text{F}}, \quad (11)$$

where σ is the cross section of the absorption of CH_3F molecules at the wavelength of the initiating radiation; I is the intensity of the initiating radiation; $n_{\text{CH}_3\text{F}^v}$ is the concentration of CH_3F molecules having absorbed m quanta; n_M is the concentration of the M component; k_1 and k_3 are the reaction rates of processes (1) and (3); and n_a is the total concentration of F and D atoms.

We will make an analysis of the initiation process and an estimate of the energy gain by taking into account conditions in the medium of a DF/CO_2 laser corresponding to the emission mode predicted in [4] with high values of the quantum yield and unit power output. These conditions, as well as the energy and time characteristics of the emission of a DF/CO_2 laser [4], are given below.

Composition of mixture	$\text{D}_2:\text{F}_2:\text{CO}_2:\text{He} = 1:3.7:0.4:3.7$
Total pressure, atm	7
Initial temperature, °K	300
Concentration of active centers, n_a , cm ⁻³	$3.7 \cdot 10^{15}$
Duration of lasing, μs	3.3
Unit power output, J/liter	333
Lasing quantum yield, f	4750

We will assume that the length of the IR radiation pulse is somewhat shorter than the length of the laser emission and equals 2 μs . Coefficient 2 in the right half of equation (11) takes into account the appearance of a second F atom as the result of reaction (2), which follows according to estimates almost instantaneously after reaction (1). Actually, based on an

FOR OFFICIAL USE ONLY

experimental study of the reactions of the fluorination of methane CH_4 and methyl fluoride CH_3F [15] it is possible to assume that the reaction rate of reaction (2) is close to that for the process $\text{CH}_3 + \text{F}_2 \rightarrow \text{CH}_3\text{F} + \text{F}$, which equals according to [15] $1.2 \cdot 10^{-13} \text{ cm}^3/\text{s}$. Then the characteristic time for reaction (2) with the concentrations of F_2 considered, of $n_{\text{F}_2} \sim 10^{20} \text{ cm}^{-3}$, equals approximately $0.1 \text{ } \mu\text{s}$, which is much shorter than the initiation length. Under the conditions considered, the characteristic times for the disappearance of CH_3F^v through channels (1) and (3) are also much shorter than the length of initiation, and the concentration of CH_3F^v can be considered quasi-steady-state. Then the kinetics for the formation of active centers are described by the equation

$$\frac{dn_a}{dt} = 2 \frac{\phi}{m} \sigma I n_{\text{CH}_3\text{F}}, \quad (12)$$

where

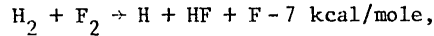
$$\phi = \frac{k_1 n_{\text{F}_2}}{k_1 n_{\text{F}_2} + \sum_M k_3^M n_M}$$

is a coefficient equal to the ratio of the rate of disappearance of excited molecules through branching channel (1) to the total rate of disappearance of CH_3F through branching channel (1) and relaxation (3) channels. Equation (12) makes it possible to estimate the intensity of the initiating IR radiation, I , required for producing a specified density of active centers, n_a , if the values of the parameters entering into it, m , ϕ , σ , and $n_{\text{CH}_3\text{F}}$ have been determined.

The number of vibrational quanta, m , required for the activation of CH_3F molecules we will determine from the following considerations. Process (1) is responsible for branching in the reaction for the fluorination of methane studied in [15]. In reacting system $\text{CH}_4 + \text{F}_2$, vibrationally excited molecules of methyl fluoride form as the result of the reaction $\text{CH}_3 + \text{F}_2 \rightarrow \text{CH}_3\text{F} + \text{F}$, whose thermal effect equals approximately 80 kcal/mole . If it is assumed by analogy with the reaction $\text{H} + \text{F}_2 \rightarrow \text{HF}^v + \text{F}$ that approximately 50 percent of the energy released in the reaction goes toward vibrational excitation of the product, then the energy of vibrations of CH_3F equals approximately 40 kcal/mole . For the purpose of achieving the same level of the vibrational excitation of CH_3F is sufficient the absorption of 13 quanta of the radiation of a CO_2 laser. This estimate represents the upper-limit estimate, since it refers to conditions when reaction (1) certainly takes place. Since reaction (1) is exothermic, then the lower-limit estimate of the required vibrational energy for CH_3F is provided by the energy for activation of the reaction between unexcited methyl fluoride and fluorine. Although the energy for activation of this reaction is not known, it hardly exceeds the energy for the activation of the reaction similar in terms of mechanism, but endothermic:

FOR OFFICIAL USE ONLY

FOR OFFICIAL USE ONLY



equal to 20 kcal/mole [16]. Thus, it is completely probable that reaction (1) will take place with the absorption of a total of six or seven or of even a lower number of photons of a CO₂ laser. In our calculations we will assume that $m = 13$, i.e., will employ the upper-limit estimate.

For the purpose of estimating coefficient ϕ we will use the value of the reaction rate of process (1) measured in [15] and experimental data on the reaction rates for the relaxation of CH₃F for different components, obtained in [12,17]: $k_1 = 10^{-14}$ to 10^{-13} cm³/s; $k_3^M = 2.2 \cdot 10^{-14}$ cm³/s (M = CH₃F, He; and the effectiveness of D₂ and F₂ are assumed to be the same); $k_3^{CO_2} = 10^{-12}$ cm³/s. The key contribution to the relaxation of CH₃F is made by relaxation in CO₂, which is accomplished by means of quasi-resonance transfer of energy. Therefore for the purpose of realizing possibly higher values of ϕ , optimal are mixtures with a high ratio of n_{F_2}/n_{CO_2} . This requirement is fulfilled in mixtures characterized by a high quantum yield of laser emission. For the conditions indicated earlier coefficient ϕ is in the range of 0.073 to 0.43. Let us assume for the sake of definiteness that the absorption cross section of CH₃ equals $3 \cdot 10^{-19}$ cm² in keeping with the estimate made, and we will assume the concentration of CH₃F to equal 10^{17} cm⁻³. Then for the purpose of producing the required concentration of active centers in 2 μ s the intensity of IR radiation should equal 0.02 to 0.12 MW/cm². It should be mentioned that the quasi-steady-state concentration of CH₃F^v molecules possessing the necessary energy for vibrational excitation under the conditions considered is much lower than the total concentration of CH₃F and equals approximately one percent of the latter in keeping with the equation

$$n_{\text{CH}_3\text{F}^v} = \frac{\sigma I}{m} \left(k_1 n_{F_2} + \sum_M k_3^M n_M \right)^{-1} n_{\text{CH}_3\text{F}}.$$

A simple calculation demonstrates that the required concentration of activated CH₃F molecules with a vibrational quanta reserve of $m \geq 13$ is reached with an average number of vibrational quanta per molecule of about three. The fact that such a level of the vibrational excitation of methyl fluoride can be actually realized under conditions of a high pressure medium is demonstrated experimentally in [11].

The analysis made makes it possible to estimate an unknown energy gain, defined as the ratio of the energy emitted by a laser to the initiation energy. Expenditures of photons for the formation of a single active center equal $m/2\phi$, and the number of emitted laser photons per single active center equals f . Then for the energy gain, K , it is possible to write

$$K = 2f\phi/m. \tag{13}$$

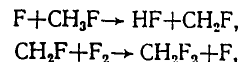
FOR OFFICIAL USE ONLY

FOR OFFICIAL USE ONLY

Substituting in (13) the values of all parameters, we find that in the variant discussed $K = 50$ to 300 . Even for values of f severalfold lower than the maximum, it is possible to create on the basis of the system suggested a chemical laser initiated by IR radiation with an energy gain not lower than 10.

The analysis made makes it possible to conclude that under conditions of a photon-branched reaction when both the absorbed and emitted photons have the same frequency, the energy gain, K , for a single amplifier stage will lie within the range of 10 to 10^3 . Even with three-stage amplification the energy of the "start" pulse will equal only 10^{-3} to 10^{-9} of the output energy, i.e., the energy requirements for the master oscillator will be very low. This makes it possible to talk about the self-contained nature of pulsed chemical lasers utilizing a photon-branched reaction.

Let us note that in analyzing the kinetic system the burnup of CH_3F was disregarded in the process of the chain reaction



taking place concomitantly with chain (4), (5). The time for the burnup of CH_3F caused by this reaction under the conditions considered is greater than $30 \mu\text{s}$, which is an order of magnitude longer than the length of the laser chemical process.

An additional contribution to branching of the chain can be made by the dissociation of vibrationally excited molecules of CH_2F_2 formed in reaction (2), the thermal effect of which equals approximately 80 kcal/mole, and the share of dissociated molecules of CH_2F_2^v under conditions of low pressures (1 to 10 mm Hg) according to [15] lies within the range of $(2 \text{ to } 5) \cdot 10^{-2}$. Although the dissociation of CH_2F_2^v at high pressures has not been studied, taking this process into account only increases the estimated value of the energy gain.

Of importance is the question of the stability of a mixture of methyl fluoride with fluorine. Experimental studies have demonstrated that the process of self-combustion of such mixtures under conditions of low pressures of the reactants is completely suppressed by dilution of the reactants with argon. Even more effective for this purpose is the addition to the mixture of CO_2 and O_2 [15]. This makes it possible to hope to achieve stability of a high-pressure working mixture of $\text{CH}_3\text{F}-\text{D}_2-\text{F}_2-\text{CO}_2-\text{He}-\text{O}_2$ for approximately 10 min, which is sufficient for conducting a laser experiment. And if longterm stability of the working mixture at high pressures is not achieved, then for the purpose of realizing the laser chemical process discussed can be used a reactor with rapid turbulent mixing of components (over a period of about 1 ms) admitted to the working space via an array of jets.

FOR OFFICIAL USE ONLY

FOR OFFICIAL USE ONLY

Bibliography

1. Basov, N.G., Markin, Ye.P., Orayevskiy, A.N. and Pankratov, A.V. DAN SSSR, 198, 1043 (1971).
2. Semenov, N.N. Preprint of IKhF AN SSSR [USSR Academy of Sciences Institute of Chemical Physics], Chernogolovka, 1975.
3. Igoshin, V.I., Nikitin, V.Yu. and Orayevskiy, KVANTOVAYA ELEKTRONIKA, 3, 2072 (1976).
4. Igoshin, V.I., Nikitin, V.Yu. and Orayevskiy, A.N. KRATKIYE SOOB-SHCHENIYA PO FIZIKE, FIAN, No 6, 20 (1978).
5. Akinfiyev, N.N., Basov, N.G., Galochkin, V.T., Zavorotnyy, S.I., Markin, Ye.P., Orayevskiy, A.N. and Pankratov, A.V. PIS'MA V ZHETF, 19, 745 (1974).
6. Galochkin, V.T., Zavorotnyy, S.I., Kosinov, V.N., Ovchinnikov, A.A., Orayevskiy, A.N. and Starodubtsev, N.F. KVANTOVAYA ELEKTRONIKA, 3, 125 (1976).
7. Balykin, V.I., Kolomiyskiy, Yu.R. and Tumanov, O.A. KVANTOVAYA ELEKTRONIKA, 2, 819 (1975).
8. Lyman, J.L. and Jensen, R.J. J. PHYS. CHEM., 77, 883 (1973).
9. Belotserkovets, A.V., Kirillov, G.A., Kormer, S.B., Kochemasov, G.G., Kuratov, Yu.V., Mashendzhinov, V.I., Savin, Yu.V., Stankeyev, E.A. and Urlin, V.D. KVANTOVAYA ELEKTRONIKA, 2, 2412 (1975).
10. Plant, T.K. and DeTemple, T.A. J. APPL. PHYS., 47, 3042 (1976).
11. McNair, R.E., Fulghum, S.F., Flynn, G.W., Feld, M.S. and Feldman, B.J. CHEM. PHYS. LETTS., 48, 241 (1977).
12. Weitz, E. and Flynn, G. J. CHEM. PHYS., 58, 2679 (1973).
13. Ambartsumyan, R.V., Gorokhov, Yu.A., Letokhov, V.S. and Makarov, G.N. ZHETF, 69, 1956 (1975).
14. Frankel, D.S., Jr. and Manuccia, T.J. CHEM. PHYS. LETTS., 54, 451 (1978).
15. Fedotov, N.G. Author's abstract of candidate's dissertation, MFTI, 1978.
16. Bokun, V.Ch. and Chaykin, A.M. DAN SSSR, 223, 890 (1975).

FOR OFFICIAL USE ONLY

FOR OFFICIAL USE ONLY

17. Stephenson, J.C. and Moore, C.B. J. CHEM. PHYS., 52, 2333 (1970).

COPYRIGHT: Izdatel'stvo Sovetskoye Radio, KVANTOVAYA ELEKTRONIKA, 1979
[83-8831]

CSO: 1863
8831

FOR OFFICIAL USE ONLY

FOR OFFICIAL USE ONLY

UDC 535.313

PROSPECTS FOR EMPLOYING POROUS STRUCTURES FOR COOLING POWER OPTICS COMPONENTS

Moscow KVANTOVAYA ELEKTRONIKA in Russian Vol 6 No 12, 1979 pp 2533-2545
manuscript received 17 Aug 79

[Article by V.V. Apollonov, P.I. Bystrov, V.F. Goncharov, A.M. Prokhorov and V.Yu. Khomich, USSR Academy of Sciences Physics Institute imeni P.N. Lebedev, Moscow]

[Text] The results are given of theoretical investigations of processes of heat and mass transfer in structures with an exposed void content, as well as the results of calculation of thermal and heat-strain characteristics of laser reflectors designed on the basis of powder and metal fiber structures, for the purpose of creating optimal designs for power optics components. The method suggested for predicting the characteristics of laser reflectors based on porous materials makes it possible to determine the optimal type and parameters of a structure guaranteeing dissipation of the required heat fluxes with permissible values of distortions of the reflecting surface.

The feasibility of employing structures with an open void content for the purpose of cooling heat-stressed laser reflectors was established for the first time theoretically and experimentally in [1,2]. An increase in the thresholds of optical failure of laser reflectors based on porous structures is made possible by the creation of a "minimum" thickness for the dividing layer (dozens of microns), the intensification of heat exchange by means of agitation of the heat transfer agent pumped through the structure, and the effect of considerable development of the surface [3]. In [4,5] it was demonstrated experimentally that the placement of special porous inserts in the tube makes it possible to increase (approximately ninefold) the effective coefficient of convective heat exchange, which according to [4] has reached about $22 \text{ W/cm}^2 \cdot \text{deg}$.

The results of tests of water-cooled laser reflectors created on the basis of structures with an open void content pointed for the first time toward the possibility of the dissipation of high heat fluxes with insignificant amounts of strain in the reflector's surface; the maximum value of the

FOR OFFICIAL USE ONLY

FOR OFFICIAL USE ONLY

density of the dissipated heat flux not resulting in failure is $q_{\max} = 8 \text{ kW/cm}^2$; with $q = 2 \text{ kW/cm}^2$ the amount of heat strain equals approximately $\lambda/20$, where $\lambda = 10.6 \mu$ [3].

A further increase in the threshold of optical failure for cooled reflecting surfaces can be achieved as the result of optimizing the parameters of the porous structure, appropriate selection of the heat transfer agent and intelligent design of the system for supplying and eliminating it. Development of such laser reflectors of an "optimal" design requires a detailed study of the processes of heat and mass transfer in porous structures, which at the present time have been inadequately investigated. Let us discuss certain aspects of this problem.

1. Temperature Field in a Porous Structure with Convective Cooling

We will calculate the temperature fields in a porous structure in a unidimensional formulation with the following assumptions: The incident radiation is uniformly distributed over the irradiated surface; the thickness of the porous layer, Δ , is considerably greater than the depth of heating, which makes it possible to consider it infinitely great ($\Delta \rightarrow \infty$) and to consider a model of a half-space; the temperature and rate of movement of the heat transfer agent through the thickness of the porous layer are constant.

Then the heat exchange equation describing the distribution of temperature over the thickness of the porous layer can be written in the form

$$\frac{d^2 t}{dx^2} = \frac{h_s}{\lambda} S_V (t - t_T), \quad (1)$$

where x is the coordinate, t and t_T are the temperatures of the material (shell) of the porous structure and the heat transfer agent, respectively; h_s is the coefficient of heat exchange between the material of the structure and the heat transfer agent; λ is the shell's heat conduction along axis X ; S_V is the heat exchange surface per unit of volume.

Equation (1) can be represented in dimensionless form:

$$\frac{d^2 \Theta}{d\bar{x}^2} = N (\Theta - 1), \quad (2)$$

where $\Theta = t/t_T$, $\bar{x} = x/d_s$ and $N = \frac{h_s d_s}{\lambda}$ are the dimensionless temperature, coordinate and parameter, respectively; d_s is the mean diameter of particles of the structure; $Nu = \frac{h_s d_s}{\lambda}$ is a modified Nusselt number characterizing the relationship between convective cooling and heat transfer on account of the shell's heat conduction; and $N' = S_V d_s$ is a dimensionless parameter characterizing the structure.

FOR OFFICIAL USE ONLY

FOR OFFICIAL USE ONLY

The boundary conditions of equation (2) can be written in the following manner:

$$\bar{x}=0; d\bar{\theta}/d\bar{x}=-\bar{N}u \bar{q} \bar{x} \rightarrow \infty; \bar{\theta} \rightarrow 1, \quad (3)$$

where $\bar{q} = q/(h_s t_T)$ is the dimensionless density of the heat flux; and q is the density of the heat flux transmitted through the dividing layer.

The solution to equation (2) with the boundary conditions in (3) has the form

$$\bar{\theta}(\bar{x}) = 1 + \bar{q} \sqrt{\bar{N}u/N'} \exp(-\sqrt{N} \bar{x}). \quad (4)$$

From (4) it follows that the rate of the drop in temperature through the thickness of the porous structure is determined by the parameter \sqrt{N} .

Let us write out some relationships needed later for the purpose of calculating the thermal characteristics of laser reflectors. The temperature of the dividing layer at the boundary of contact with the porous base ($\bar{x} = 0$) equals:

$$\bar{\theta}_p = 1 + \bar{q} \sqrt{\bar{N}u/N'}. \quad (5)$$

The maximum density of the heat flux eliminated from the reflector in the convective cooling mode, from the condition for the equality of $\bar{\theta}_r$ and the boiling point, $\bar{\theta}_s$, of the heat transfer agent, at the appropriate pressure ($\bar{\theta}_r \approx \bar{\theta}_s$) equals:

$$\bar{q}_{\max} = (\bar{\theta}_s - 1) \sqrt{N'/\bar{N}u}. \quad (6)$$

The degree of intensification of heat exchange in a porous structure as the result of agitation of the flow and development of the surface is determined by the coefficient K_{in} , which characterizes the ratio of the amount of heat dissipated by the heat transfer agent in the structure considered to the amount of heat which would be dissipated directly from the cooled surface of the dividing layer by the heat transfer agent when flowing in a slit channel of depth Δ :

$$K_{RH} = q/h_{\Delta}(t_{x=0} - t_T),$$

where h_{Δ} is the coefficient of convective heat exchange when the heat transfer agent flows in a slit-type gap of magnitude Δ [6]. For example, for a turbulent mode of flow of the heat transfer agent the equation for determining the Nusselt number, Nu_{Δ} , has the form

FOR OFFICIAL USE ONLY

$$Nu_{\Delta} = 0,023 Re^0,8 Pr^0,4,$$

where Re and Pr are the Reynolds and Prandtl numbers.

Let us introduce the coefficient of the intensification of heat exchange on account of agitation of the flow, $K_T = h/h_s$, where h_s is calculated from the condition of constancy of the rate of flow of the heat transfer agent circulating through the reflector. Then K_{in} , depending on the type and parameters of the structure, as well as on the thermophysical properties of the heat transfer agent, is computed thus:

$$K_{in} = K_0 K_T, \quad (7)$$

where $K_0 = q/h_s(t_{x=0} - t_T) = (N'/Nu)^{1/2}$ is the fin-effect cooling coefficient of the cooled surface of the dividing layer.

From equation (4) we find the depth of heating of the structure, determining the minimum possible thickness of the porous layer, assuming by a convention that heating terminates at coordinate $\bar{\Delta} = x/d_s$, where the temperatures of the shell and heat transfer agent differ by one percent:

$$\bar{\Delta} = N^{-1/2} \ln 10^2 \bar{q} (\bar{N}u/N')^{1/2}. \quad (8)$$

In the case of dissipation of maximum densities of heat flux the depth of heating equals

$$\bar{\Delta}_{max} = N^{-1/2} \ln 10^2 (\Theta_s - 1). \quad (9)$$

Thus, the equations obtained, (4) to (9), make it possible to calculate the heat fields and thermal characteristics of cooled laser reflectors. In combination with expressions describing the hydrodynamics of the flow, they are the basis for optimizing the parameters of porous structures ensuring minimum heat strains in the reflecting surface, or, if this is necessary, the maximum heat fluxes dissipated in convective cooling.

2. Convective Heat Exchange in a Porous Structure

The mode of flow of a heat transfer agent in porous materials of interest for power optics is an intermediate one between the laminar and developed turbulent modes; here calculation of the coefficient of heat exchange between the shell and the heat transfer agent is very difficult in spite of numerous experimental data. The most complete survey of experimental investigations of heat exchange in porous materials, chiefly for gaseous heat transfer agents, is given in [7], where in addition to dimensionless

FOR OFFICIAL USE ONLY

FOR OFFICIAL USE ONLY

equations for calculating heat exchange coefficients are presented a procedure for processing experimental data and a form for the representation of decisive dimensionless numbers.

But the lack of a unified approach to processing experimental results and the impossibility of a precise determination of such important characteristics as S_V , d_s , etc. hinder the employment of the equations in [7] for calculating the heat exchange of trickling fluids in different types of porous structures with geometrical parameters varying over a wide range. Therefore these relationships can be recommended only as a first approximation for calculation of the volumetric coefficient of heat exchange in structures identical to the experimental, and as applied to gaseous coolants.

It has become generally acknowledged that the dimensionless equation for intrapore convective heat exchange for gases and trickling fluids has the form [7]

$$Nu = c (Re Pr)^n, \quad (10)$$

where c and n are constants depending only on the structural characteristics of the porous material.

Based on the experimental data in [7-10], we made an analysis of the dependence of c and n on the structural characteristics of porous materials for which the latter were known with sufficient certainty; it was established as a result that c and n depend chiefly on the volumetric void content, P_V .

Thus, equation (10) for the dimensionless Nusselt number taking into account the correlation expressions $c(P_V)$ and $n(P_V)$ makes it possible to calculate the coefficient of convective heat exchange in a porous material.

3. Hydrodynamics of Single-Phase Flow in a Porous Structure

The temperature field and heat straining of the reflector are determined to a considerable extent by the rate of flow of the heat transfer agent pumped through the porous layer, and this rate depends on hydrodynamic characteristics and the conditions for supplying and discharging the heat transfer agent. A great number of experimental studies, a survey of which is given in [7,8], are devoted to an investigation of hydrodynamic characteristics in the flow of a single-phase heat transfer agent in porous materials, chiefly in the region of $P_V \leq 0.5$. The equations suggested by different authors can be used for the calculation of the hydrodynamics of a flow in materials having a structure identical to that of the models investigated.

Generally the hydrodynamics of a flow in porous materials are described by a modified D'Arcy equation (a Dupuit-Reynolds-Forcheimer equation [11-13]):

FOR OFFICIAL USE ONLY

FOR OFFICIAL USE ONLY

$$-\frac{dp}{dx} = \alpha\mu u + \beta\rho u^2, \quad (11)$$

where p is the pressure of the flow; u is the filtering rate, equal to the ratio of the unit bulk rate of flow of the heat transfer agent, V , to the density, ρ ; α and β are the viscous and inertial drag coefficients, respectively; and μ is the coefficient of dynamic viscosity of the heat transfer agent.

From equation (11) we get the equation for the coefficient of frictional drag, C_f , in the form

$$C_f = 2/Re + 2, \quad (12)$$

where $C_f = -2(dp/dx)\rho/G^2\beta$ and $Re = G\beta/\mu\alpha$ (β/α is the characteristic dimension).

The practical utilization of equation (12) for the purpose of calculating the hydrodynamics of a flow in different types of porous materials whose structural characteristics vary over a wide range is difficult because of the lack of necessary information on coefficients α and β , which as a rule are determined experimentally.

In [14] is given a somewhat different approach to the calculation of C_f : Selected as the characteristic dimension is \sqrt{K} , where K is the penetrability factor characterizing the hydrodynamics of the flow of a stream in the D'Arcy mode ($Re_{\sqrt{K}} = G\sqrt{K}/\mu$); then

$$C_f = 2(1/Re_{\sqrt{K}} + c)/c. \quad (13)$$

The relationship between coefficients α and β and parameters c and K can be represented in the form $\alpha = 1/K$, $\beta = c/\sqrt{K}$.

As demonstrated in [14,15], parameter c is a universal constant for porous structures of the same type, e.g., for all materials made of metallic powders with particles of spherical shape or close to it, $c \approx 0.55$, and for materials made of powders of random shape, $0.45 < c < 0.566$. Therefore, below in calculating hydraulic characteristics of structures we will assume that $c = 0.55$, although in our case this gives a somewhat too high value of the coefficient of friction.

Studies conducted with fibrous materials, foam plastics and structures consisting of layers of particles of random form [14,15] have demonstrated

FOR OFFICIAL USE ONLY

FOR OFFICIAL USE ONLY

that parameter c for them is relatively low. This is explained by the fact that c , characterizing the percentage of inertial losses, depends chiefly on the nature of the wake formed behind solid particles when streamlined by a flow, and the wake is determined by the type of porous structure.

The presence in metal fiber structures of free ends which additionally agitate the flow results in an increase in c ; thus, for relatively short fibers, $l/d = 50$ to 100 and $c \approx 0.132$ [14].

The penetrability factor, K , being a structural characteristic of a porous material, does not depend on the conditions of flow and is determined experimentally from D'Arcy's law. In connection with the development of studies in the area of heating pipes at the present time, there is a sufficiently great number of experimental data for determining K both for powder and metal fiber structures [8,16].

From the experimental data in [17] the dependence of the penetrability factor of metal fiber structures on the volumetric void content has the form:

$$K = A\Pi_v^m, \quad (14)$$

where A and m are coefficients depending on the relative length of fibers, l/d [16]. Similar expressions can be obtained for powder materials, too.

In addition, the penetrability factor is calculated from the well-known Kármán-Kozeny equation:

$$K = \phi\Pi_v^2 d_s^2 / (1 - \Pi_v)^3 \approx \Pi_v^2 / 5S_v, \quad (15)$$

where ϕ is a constant depending on the structure.

The equations presented, (13) to (15), have been used for determining the hydraulic characteristics of power optics components designed on the basis of porous materials made of metal powders and metal fiber structures.

4. Influence of Conditions for Supply and Discharge of Heat Transfer Agent on Hydraulic Characteristics of a Reflector

Usually in cooled laser reflectors the supply and discharge of the heat transfer agent for the porous structure are carried out via staggered channels evenly distributed over the cooling surface, which are made in the form of slits or holes. With the slit form of delivery are made possible a more uniform velocity field for the heat transfer agent and a minimum drop in the pressure required to pump it, and with supply and discharge of the staggered hole variety there can take place considerable nonuniformity of the velocity field with spreading of the flow in radial directions.

FOR OFFICIAL USE ONLY

FOR OFFICIAL USE ONLY

This results in considerable losses of pressure in circulation of the heat transfer agent, which are taken into account by coefficient K_g ; in this case the total pressure drop in the porous layer equals

$$\Delta P = \Delta p K_g, \quad (16)$$

where Δp is the pressure drop with a uniform velocity field.

On the assumption of uniform injection (flowoff) of the heat transfer agent in radial directions in delivery (discharge) zones bounded by the region $r_0 \leq r \leq s/2$ (where s is the spacing between staggered holes and r_0 is the radius of the hole), coefficient K_g characterizing the influence of collector effects on hydraulic drag in movement of the flow in a porous layer can be represented in the form:

$$K_g = \frac{F}{\pi s^2 n (1-a)} \frac{cG (1/a - 1) / \pi n \rho s \Delta - (v/\sqrt{K}) \ln a}{v/\sqrt{K} + cv}. \quad (17)$$

Here G is the bulk rate of flow of the heat transfer agent; F is the area of the irradiated surface; n is the number of channels for supplying (discharging) the heat transfer agent; and $a = 2r_0/s$ is the relative spacing between holes. It is obvious from (17) that K_g depends both on the geometrical characteristics of the system for delivering and discharging the heat transfer agent (on a) and on G ; with an increase in a and G coefficient K_g increases. Thus, K_g characterizes the structural ideality of the system for distributing and collecting the heat transfer agent of a cooled reflector.

With known K_g the total pressure drop in the porous layer is calculated from equation (16) taking into account the following expression for the calculation of Δp :

$$\Delta p = v \rho s (1-a) (v/\sqrt{K} + cv) / \sqrt{K}, \quad (18)$$

where $v = Gs/(\rho F \Delta)$ is the filtering rate of the heat transfer agent.

5. Heat Conduction of a Porous Material

As applied to questions relating to the cooling of power optics components, it is of interest to investigate the shell heat conduction of a porous material without taking into account the heat conduction of the heat transfer agent pumped through. In [8,17] are generalized the results of numerous experimental investigations of the heat conduction of materials of different structures and it is demonstrated that the effective heat conduction depends not only on the volumetric void content, but also on such factors

FOR OFFICIAL USE ONLY

FOR OFFICIAL USE ONLY

as the material's tendency to cake, the size and shape of the original particles, the technology for compacting and sintering, etc., which results in a wide variance of data and hinders the generalization of results.

In practice data are generalized in the form of dependences $\lambda^v(P_v)$ for samples made according to a unified technology from the same type of material. An analysis of experimental results has shown that for the purpose of calculation over a wide range of values of the void content of powder materials can be used Odolevskiy's equation [8]:

$$\tilde{\lambda} = \lambda_k(1 - \Pi_v)/(1 + \Pi_v), \quad (19)$$

where λ_k is the heat conduction of a compacted material.

The effective heat conduction of metal fiber felt structures can have considerable anisotropy depending on the direction of felting. Thus, on the basis of [17], λ^v is generalized by the following equations:

$$\tilde{\lambda} = \lambda_k(1 - \Pi_v) \exp(-\Pi_v), \quad (20a)$$

$$\tilde{\lambda} = \lambda_k(1 - \Pi_v)^2, \quad (20b)$$

where λ^v is the effective heat conduction in directions parallel (20a) and perpendicular (20b) to the felting plane. In the latter case can be used the equation

$$\tilde{\lambda} = \lambda_k(1 - \Pi_v)^3. \quad (21)$$

Equations (20b) and (21) satisfactorily approximate the experimental data and can be used in determining the thermal characteristics of cooled laser reflectors designed on the basis of metal fiber structures. Here equation (20b) describes the upper limit of experimental data (the optimistic estimate) and (21) the lower (pessimistic estimate).

6. Estimation of the Amount of Heat Straining of the Optical Surface

Generally, the heat strains of a reflector are calculated from the temperature field of the dividing layer and the porous base and the known conditions for fastening them. A precise solution to this heat strength problem under real conditions of the irradiation of a reflector presents great difficulties.

For the purpose of estimating slight distortions of an optical surface characteristic of straining of power optics components, it is possible to

FOR OFFICIAL USE ONLY

FOR OFFICIAL USE ONLY

make an assumption regarding the free expansion of the porous base and dividing layer in keeping with the temperature fields. Then the heat straining of a reflector surface, W , is the sum of the expansions of the dividing (thickness of Δ_r) and porous (thickness of Δ) layers:

$$W = \alpha_p \Delta_p t_r^{1/2} (\theta_1 + \theta_2) - \theta_0 + \alpha_n \Delta t_r [(1 - \theta_0) + \bar{q} d_s / (N' \Delta)], \quad (22)$$

where α_r and α_p are the temperature coefficients of linear expansion of the dividing and porous layers, respectively; $\theta_1 = T_1/t_T$ is the dimensionless temperature; t_0 is the temperature of the heat transfer agent at the inlet into the reflector; and t_1 and t_2 are the temperatures of the outer and inner surfaces of the dividing layer, respectively.

From equation (22) it follows that the higher the rate of flow of the heat transfer agent ($\theta_0 \rightarrow 1$), the lower is W . Maximum strains of the optical surface are realized in the area of drainage of the heat transfer agent from the porous layer, whereby the amount of heating of the heat transfer agent when it is supplied through slit-type channels is

$$\Delta t_r = qF / GC_T,$$

where C_T is the heat capacity of the heat transfer agent.

i. Results of Calculations of Thermal Characteristics of Reflectors

The equations arrived at above, describing the processes of heat and mass transfer in a porous structure, were employed by us for the purpose of calculating the characteristics of cooled laser reflectors with a system for supplying and discharging the heat transfer agent in the form of evenly (with a spacing of s) staggered holes; the distribution of the heat load over the surface of the reflector was assumed to be uniform.

In fig 1 is given the qualitative dependence of straining on the maximum density of the dissipated heat flux (variable P_V with constant d_s) for two isolated zones of a reflector corresponding to regions for the injection, $W_1(q_{\max})$, and outflow, $W_2(q_{\max})$, of the heat transfer agent. By varying the mean size of the grain, \bar{v}_s , (or the diameter of the fiber), it is possible to plot a family of curves characterized by a constant value of d_s and a variable void content, P_V , for reflectors with an identical type of capillary structure. The curves are plotted upon the condition of constancy of the pressure drop of the heat transfer agent and taking into account its heating in the porous layer, and the temperature of the heat transfer agent at the inlet is assumed to equal the temperature of the final finish of the reflector.

Straining of the optical surface in the zone of outflow of the heat transfer agent equals $W_2 > W_1$; therefore, of decisive significance for selection of the structural characteristics of a porous material is curve 2, and the difference between curve 1 and 2 characterizes the degree of

FOR OFFICIAL USE ONLY

FOR OFFICIAL USE ONLY

ideality of the cooling system. These curves represent envelopes of the working heat strain characteristics of a family of reflectors with a specific type of structure.

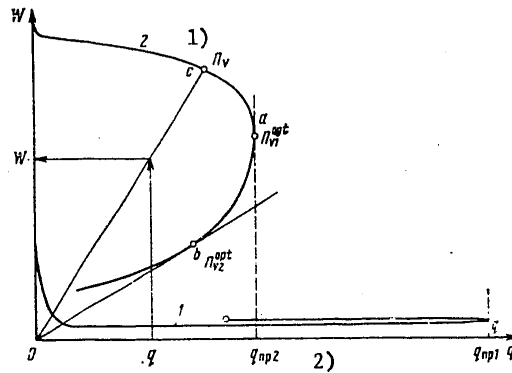


Figure 1. Qualitative Dependence of Heat Straining on Maximum Density of Dissipated Heat Flux for Two Zones of a Reflector Corresponding to Regions of Injection (1) and Outflow (2) of the Heat Transfer Agent

Key:

1. P_V

2. q_{pr2}

The working characteristic of a reflector with a predetermined void content of the structure, P_V , is obtained by connecting by a straight line point C with the origin. Point C corresponds to the maximum density of the heat flux dissipated in the convective cooling mode, and straight line segment OC represents the dependence of heat distortions of the reflecting surface on the heat load.

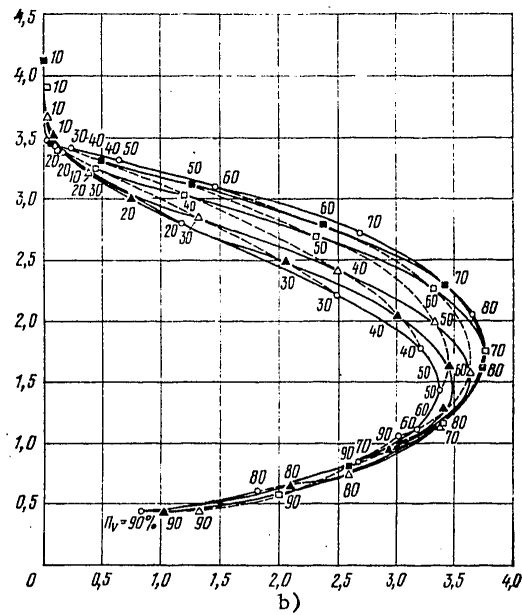
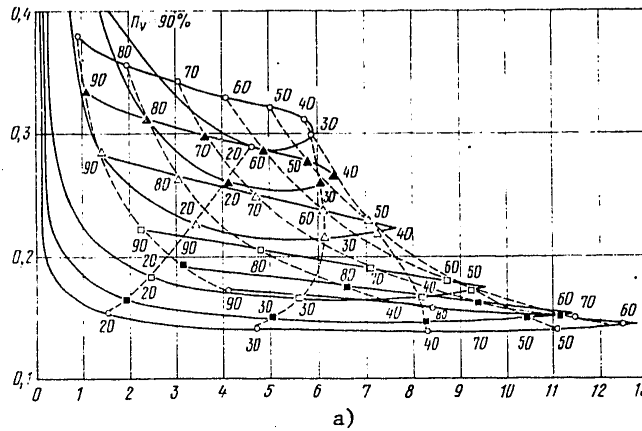
Generally on curve 2 it is possible to isolate two points: A, corresponding to the optimal void content, P_{V1}^{opt} , with which is ensured the dissipation of maximum densities of heat flux for a selected grain size, pressure drop of the heat transfer agent and conditions for supplying and discharging it, and B (the point of contact of curve 2 with the straight line from the center of the coordinates), corresponding to the void content, P_{V2}^{opt} , with which for a specific porous structure are realized optimal heat distortions of the reflecting surface.

Selection of the material and key parameters of the structure (d_s and P_V) should be done on the basis of comparing family of curves 2 with

FOR OFFICIAL USE ONLY

FOR OFFICIAL USE ONLY

opportunities for producing porous materials of the required structure and for creating the dividing layer with them.



[Continuation and caption on following page]

FOR OFFICIAL USE ONLY

FOR OFFICIAL USE ONLY

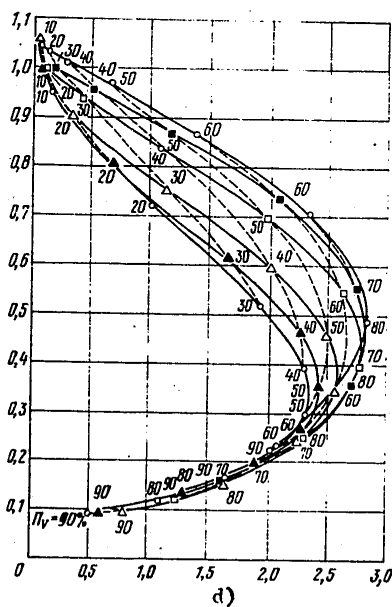
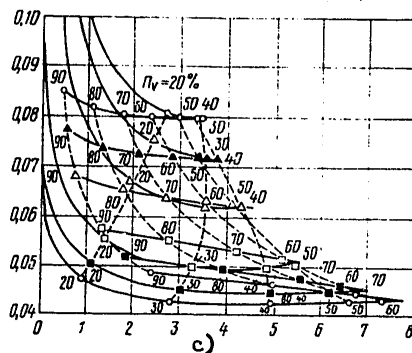
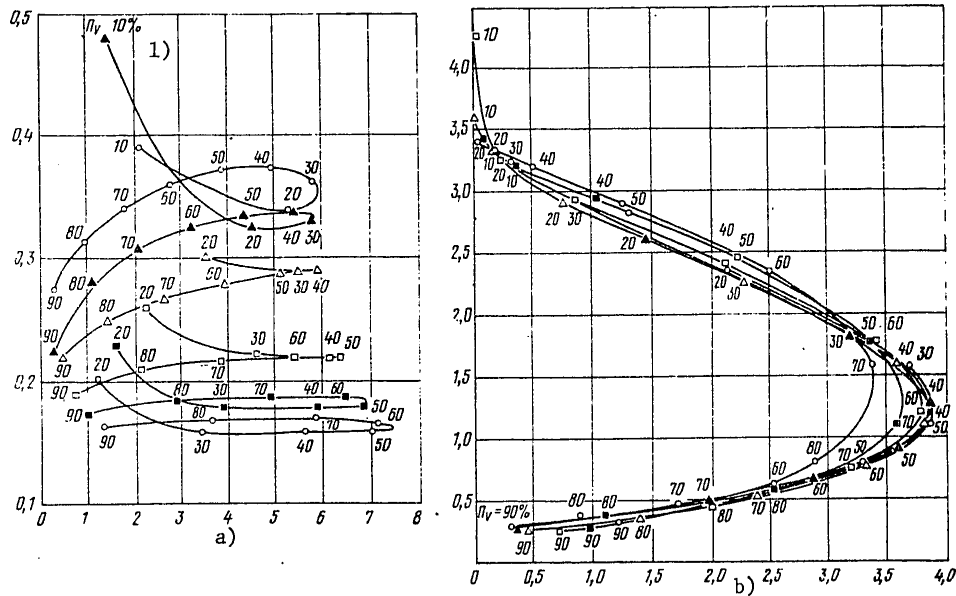


Figure 2. Nomograms of Heat Strain Characteristics for a Family of Water-Cooled Reflectors Based on Porous Structures Made from Copper (a and b) and Molybdenum (c and d) Powders for the Injection Zone (a and c) and Discharge Zone (b and d)
 [Continued on following page]

FOR OFFICIAL USE ONLY

FOR OFFICIAL USE ONLY

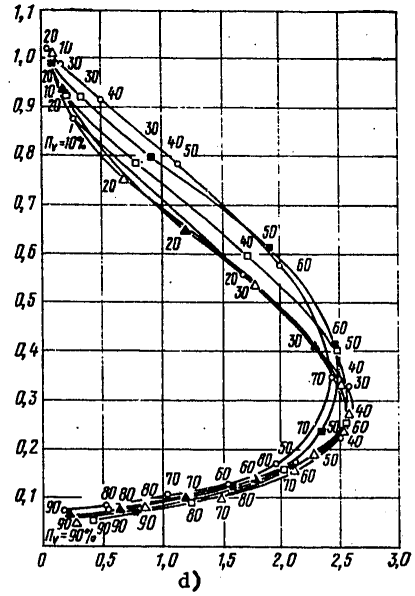
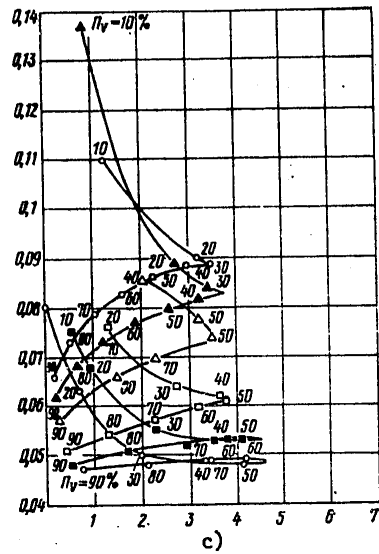
The points in this and remaining figures correspond to the following diameters of particles or of the felt: white dots--20, black squares--30, white squares--50, white triangles--100, black triangles--150 and white dots [as published]--200 microns



[Continuation and caption on following page]

FOR OFFICIAL USE ONLY

FOR OFFICIAL USE ONLY



[Caption on following page]

FOR OFFICIAL USE ONLY

FOR OFFICIAL USE ONLY

Figure 3. Nomograms of Heat Strain Characteristics of Family of Water-Cooled Reflectors Based on Porous Structures Made from Copper (a and b) and Molybdenum (c and d) Felt, for the Injection Zone (a and c) and Discharge Zone (b and d)

Key:

1. $P_V = 10$ percent

In figs 2 and 3 are given the results of numerical calculations of the heat strain characteristics of a series of water-cooled reflectors with porous structures made from the widely used copper (fig 2a and b) and molybdenum (fig 2c and d) powders, illustrating the capabilities of the method. The mean grain diameter and volumetric void content varied over the range of $20 \mu \leq d_s \leq 200 \mu$ and $0.1 \leq P_V \leq 0.9$.

From fig 2 it is obvious that the limiting densities of heat flux equaled: in the zone for supplying the heat transfer agent, $q_{pr1} = 12.8 \text{ kW/cm}^2$, and in the zone for discharging it, $q_{pr2} = 3.75 \text{ kW/cm}^2$, whereby $W_1 = 0.1$ to 0.4μ and $W_2 = 0.4$ to 3.5μ . In the region of maximum densities of heat fluxes $W_2 = 1.5$ to 2μ , which in the majority of cases is substantially higher than the maximum permissible straining of reflectors for CO_2 lasers.

With an increase in the rate of flow of the heat transfer agent (fig 2b) W_2 can be reduced drastically by using materials with a high volumetric void content (0.7 to 0.8) and by changing to a larger grain size. Here $q_{max} \sim 2 \text{ kW/cm}^2$ with $W = 0.5 \mu$. The creation of structures with $P_V > 0.75$ from powder materials while observing the necessary requirements for power optics is very difficult. With a reduction in void content to realistic values of approximately 0.6, the dissipated densities of heat flux with deformation of approximately 0.5μ equal approximately 1.4 kW/cm^2 . Let us note that an increase in the rate of flow of the heat transfer agent is achieved also by means of an intelligent design for the delivery and discharge system to ensure a more uniform distribution of the heat transfer agent over the cooling surface.

It is obvious from fig 2c and d that the employment of porous molybdenum makes it possible to reduce approximately fourfold the level of heat strains of the reflecting surface both in the first and in the second zones, whereby q_{pr} is somewhat lowered: $q_{pr1} = 7.8 \text{ kW/cm}^2$ and $q_{pr2} = 2.8 \text{ kW/cm}^2$. For this structure (fig 2c) with the realization of maximum dissipated fluxes the heat strains which originate lie below the characteristic optical failure thresholds of reflectors for CO_2 lasers. For example, a structure with $P_V = 83$ percent and $d_s = 20 \mu$ enables dissipation of $q_{max} = 2.8 \text{ kW/cm}^2$ with $W = 0.45 \mu$. With an increase in the rate of flow of the heat transfer agent (fig 2b), $W_2 + W_1$, but q_{max} is thereby reduced. In this region the level of dissipated heat fluxes can be raised

FOR OFFICIAL USE ONLY

FOR OFFICIAL USE ONLY

as the result of using materials with larger grain sizes; for example, a molybdenum powder structure with $P_v = 60$ percent and $v = 20 \mu$ makes possible dissipation of $q_{\max} = 2.1 \text{ kW/cm}^2$ with $W = 0.23 \mu$.

In fig 3 are presented the heat strain characteristics of reflectors with porous structures made from copper (fig 3a and b) and molybdenum (fig 3c and d) felt. It is obvious from fig 3a and c that a changeover to metal fiber structures results in a substantial (approximately 1.7-fold) reduction in q_{pr} , which is related to the reduction in the effective heat conduction of these structures as compared with powder structures.

In zones for discharge of the heat transfer agent (fig 3b and d) the limiting densities of heat flux lie at the same level as for reflectors with powder structures, but an increase in the rate of flow of the heat transfer agent results in a stronger dependence of W on P_v and in lower sensitivity of W to the diameter of the original fibers. Here strains corresponding to q_{pr} prove to be approximately twofold less than with powder structures: For reflectors made of copper $W = 1.2 \mu$ with $q_{pr} = 3.9 \text{ kW/cm}^2$, and of molybdenum, $W = 0.3 \mu$ with $q_{pr} = 2.6 \text{ kW/cm}^2$.

For reflectors with a copper fiber structure the densities of heat flux which can be realized with $W = \lambda/20$ (where $\lambda = 10.6 \mu$) equal 2.4 kW/cm^2 , which is higher than the corresponding level of q_{\max} for powder materials. Thus, the employment of metal fiber structures for the purpose of creating on their basis power optics components is quite promising; for example, for a structure made of molybdenum fibers with a diameter of 100 to 200 μ and a void content of 50 to 60 percent, $q_{\max} = 2.2 \text{ kW/cm}^2$ with $W \approx 0.15 \mu$; in addition, the possibility of producing materials with high values of $P_v = 70$ to 80 percent makes it possible to create optimal designs of reflectors.

8. Comparison of Theoretical and Experimental Results

We compared the results of a calculation of heat straining of the reflecting surface of a laser reflector based on a porous material made out of a copper powder with the experimental data in [3].

In fig 4 are given the results of experimental investigations of heat straining of a water-cooled reflector as a function of the density of the dissipated heat flux, as well as the results of a calculation of maximum heat strain characteristics in the zone of discharge of the heat transfer agent for a series of reflectors with a void content of 55 to 70 percent. The straight lines represent calculated characteristics of the tested reflector for extreme void content values of 60 and 62 percent. It is obvious that there is good agreement of the theoretical and experimental data.

In fig 4b is illustrated a calculation of the heat strain characteristic of this series of reflectors in the zone of delivery of the heat transfer

FOR OFFICIAL USE ONLY

FOR OFFICIAL USE ONLY

agent, which, as occurred in fig 4a, was arrived at on condition of equality of the temperature of the cooled surface of the dividing layer to 100°C. From fig 4b it follows that $q_{max} = 8 \text{ kW/cm}^2$, which is in good agreement with the experimental data.

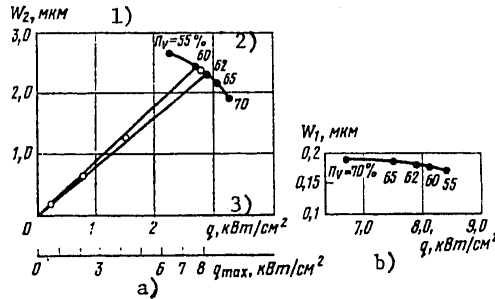


Figure 4. Heat Strain Characteristics of a Series of Water-Cooled Reflectors Based on Porous Structures Made of a Copper Powder: Injection Zone (a) and Discharge Zone (b) (black dots--theoretical; white dots--experimental)

Key:

- 1. μ
- 2. $P_v = 55$ percent
- 3. q , kw/cm^2

In conclusion, let us note that the method discussed for predicting the thermal and strain characteristics of laser reflectors based on porous materials makes it possible to determine the optimal type and parameters of a structure ensuring dissipation of the necessary heat fluxes with permissible values of distortion of the reflecting surface. The results of theoretical and experimental investigations confirm that water-cooled laser reflectors with a porous structure have a high optical failure threshold. As new experimental data are accumulated on convective heat exchange and on the hydrodynamics of flows in porous structures these can be incorporated sufficiently easily into the calculation algorithm.

Bibliography

1. Apollonov, V.V., Barchukov, A.I., Prokhorov, A.M. and Khomich, V.Yu. "Tezisy dokl. IV Vsesoyuz. soveshchaniya po nerezonansomu vzaimodeystviyu opticheskogo izlucheniya s veshchestvom" [Theses of Papers at the Fourth All-Union Conference on Non-Resonance Interaction of Optical Radiation with Matter], Leningrad, GOI, 1978, p 31.

FOR OFFICIAL USE ONLY

FOR OFFICIAL USE ONLY

2. Apollonov, V.V., Barchukov, A.I., Borodin, V.I., Bystrov, P.I., Goncharov, V.F., Ostrovskaya, L.M., Prokhorov, A.M., Rodin, V.N., Trushin, Ye.V., Khomich, V.Yu., Tsy-pin, M.I., Shevakin, Yu.V. and Shur, Ya.Sh. KVANTOVAYA ELEKTRONIKA, 5, 1169 (1978).
3. Apollonov, V.V., Barchukov, A.I., Borodin, V.I., Bystrov, P.I., Goncharov, V.F., Ostanin, V.V., Ostrovskaya, L.M., Prokhorov, A.M., Rodin, V.N., Trushin, Ye.V., Khomich, V.Yu., Tsy-pin, M.I., Shevakin, Yu.F. and Shur, Ya.Sh. PIS'MA V ZHTF, 4, 1193 (1978).
4. Megerlin, F.Ye., Merfi, R.V. and Berles, A.Ye. TEPLOPEREDACHA, SER. S, No 2, 30 (1974).
5. Polyayev, V.M., Morozova, L.L., Kharybin, E.V. and Avraamov, N.I. IZV. VUZOV, SER. MASHINOSTROYENIYE, No 2, 86 (1976).
6. Isachenko, V.P., Osipova, V.A. and Sukomel, A.S. "Teplotperedacha" [Heat Transfer], Moscow, Energiya, 1969.
7. Mayorov, V.A. TEPLOENERGETIKA, No 1, 64 (1978).
8. Belov, S.V. "Poristyye metally v mashinostroyeni" [Porous Metals in Machine Building], Moscow, Mashinostroyeniye, 1976.
9. Keys, V.M. and London, A.L. "Kompaktnyye teploobmenniki" [Compact Heat Exchangers], Moscow, Energiya, 1967.
10. Lykov, A.V. "Teplomassobmen" [Heat and Mass Exchange], Moscow, Energiya, 1978.
11. Dupuit, J. "Etudes théoriques et pratiques sur le mouvement des eaux" [Theoretical and Practical Studies on the Motion of Water], Paris, 1863.
12. Reynolds, O. "Papers on Mechanical and Physical Subjects," Cambridge University Press, 1900.
13. Forcheimer, P. "Wasserbewegung durch Boden" [Movement of Water Through Soil], Z. VEREINES DEUTSCHER INGENIEURE, 45, (1901).
14. Biverz, G.S. and Sperrou, Ye.M. PRIKLADNAYA MEKhanIKA, SER. YE, 36, No 4, 59 (1969).
15. Biverz, G.S., Sperrou, Ye.M. and Rodenz, D.Ye. PRIKLADNAYA MEKhanIKA, SER. YE., 40, No 3, 12 (1973).
16. Semena, M.G., Kostornov, A.G., Gershuni, A.N., Moroz, A.L. and Shevchuk, M.S. TEPLOFIZIKA VYSOKIKH TEMPERATUR, 13, 162 (1975).

FOR OFFICIAL USE ONLY

17. Semena, M.G., Kostornov, A.G., Zaripov, V.K., Moroz, A.L. and Shevchuk, M.S. INZH. FIZ. ZHURN., 31, 581 (1976).

COPYRIGHT: Izdatel'stvo Sovetskoye Radio, KVANTOVAYA ELEKTRONIKA, 1979
[83-8831]

CSO: 1862
8831

FOR OFFICIAL USE ONLY

FOR OFFICIAL USE ONLY

UDC 621.375.826

RELATIONSHIP BETWEEN THE STATISTICS OF LASER DAMAGE TO SOLID TRANSPARENT MATERIALS AND THE STATISTICS OF STRUCTURAL DEFECTS

Moscow KVANTOVAYA ELEKTRONIKA in Russian Vol 6 No 12, 1979 pp 2590-2596
manuscript received 6 Apr 79

[Article by Yu.K. Danileyko and A.V. Sidorin, USSR Academy of Sciences
Physics Institute imeni P.N. Lebedev, Moscow]

[Text] The problem is discussed of the statistics of bulk laser damage under the effect of focused beams. A new method is suggested for an experimental determination of the defect distribution function from failure thresholds in the low-threshold region. The method is based on an investigation of fluctuations in the distance from the focal point of the lens to the fracture most remote from it. Experiments are performed on single crystals of silicon and gallium arsenide by utilizing the radiation of a pulsed CO₂ laser. A conclusion is drawn regarding the applicability of the procedure to investigation of defects of condensed media.

1. Introduction

As is known, real optical materials possess a considerable amount of different kinds of structural defects of the foreign-phase inclusion type, cluster-type pile-ups, inhomogeneities in composition, etc. [1]. These formations can initiate laser failure and result in considerable lowering of the threshold. The concentration of these defects even in highly pure and ideal materials can be high--right up to 10^9 cm^{-3} [1,2]. It is precisely the existence of such high concentrations of defects which results in the fact that high failure thresholds (10^{10} to 10^{11} W/cm^2) characteristic of critical failure mechanisms are realized only in volumes of approximately 10^{-10} to 10^{-9} cm^3 . With an increase in the extent of interaction between high-power electromagnetic radiation and the material there occurs a lowering of the failure threshold, associated with an increase in the probability of inclusions with a low failure threshold entering the interaction region (the so-called dimensional effect) [3]. This reduction depends on the features of the defects present in the optical material and can vary noticeably from sample to sample.

FOR OFFICIAL USE ONLY

FOR OFFICIAL USE ONLY

Questions relating to predicting the laser resistance of materials containing inhomogeneities are complicated for two reasons. First there is the almost total absence of methods of determining the dimensions, structure and chemical composition of microdefects. Second there is the impossibility of constructing quantitative theories of laser failure without complete information, including statistical, on the magnitude and mechanism of the absorption of light radiation in the region of inhomogeneities. It is precisely for this reason that it is of interest to investigate the statistics of laser failure. This interest is based not only on obtaining statistical data on the failure thresholds of a material, but also on the possibility of obtaining information on the mechanism of failure and the characteristics of defects.

Since the statistics of laser failure in defects are determined totally by the distribution function of threshold intensities of failure, $f(I)$, the purpose of this study has been to develop methods of investigating it experimentally. Knowledge of function $f(I)$ in the region of high intensities is important in connection with explaining the role of critical mechanisms (cumulative or multi-photon ionization) in the failure of transparent materials. Meanwhile the form of function $f(I)$ in the region of low intensities determines the real optical strength, i.e., not the local failure threshold, but the threshold characteristic of a large volume. In this study we will be interested only in the low-threshold portion of distribution function $f(I)$.

2. Choice of Investigation Procedure

Let us consider an optical material containing defects randomly distributed over its volume. Let each defect be characterized by its own failure threshold. In this case under the effect of laser radiation the morphological pattern of failure will have the form of individual foci the local concentration of which is determined by the intensity of radiation and the function for the distribution of defects by failure threshold. However, it proves to be impossible to determine its form by the direct measurement of the concentration of failures, since the spatial distribution of the intensity of radiation in the interaction region is unknown. This is associated with the unknown law for the attenuation of radiation in the direction of propagation resulting from screening by the failures which occur.

Actually, as our experiments have demonstrated, in focusing the radiation of a CO_2 laser with power approximately an order of magnitude greater than the threshold onto the bulk of a sample of silicon, in it originates a region of failure measuring approximately 10^{-7} cm^3 and containing about 100 individual microfoci [4]. In spite of the fact that the intensity resulting from focusing should have increased as the focal point was neared, the reduction in the concentration of microfractures in the direction of propagation testifies to the opposite. This has been confirmed also by the strong "cutoff" of radiation passing through the sample.

FOR OFFICIAL USE ONLY

FOR OFFICIAL USE ONLY

Thus, information regarding the distribution function of defects in terms of the failure threshold can be obtained only from magnitudes not subject to the influence of the "cutoff." As such a magnitude we will employ the distance from the focal point of the lens to the seat of failure at the maximum distance from it.

3. Theoretical Analysis

Let a cylindrical beam of power P_0 with a uniform distribution of intensity, I , in terms of cross section be focused on a medium containing structural microdefects with a concentration of n_0 and distributed randomly and independently over the bulk of the sample. We will assume that a great number of defects ($Vn_0 \gg 1$) are contained in the region of interaction discussed, of length z_0 , and having in our case the shape of a cone (fig 1) with a volume equal to $V = (1/3)Az_0^3$ ($A = \pi \tan^2 \alpha$ and 2α is the angle at the apex of the cone). If it is assumed that each of them is characterized by its own threshold degree of failure, then it is possible to introduce function $f(I)$, representing the distribution density for the magnitude of the threshold intensity and normalized in the following manner:

$$\int_0^\infty f(I) dI = n_0.$$

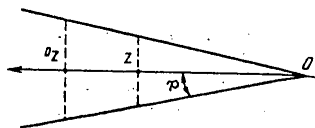


Figure 1. Geometry of Focusing of Laser Radiation

In this case $P(z)$ --the probability that between cross sections z and z_0 there will occur but a single seat of failure--is determined by the equation [5]:

$$P(z) = \frac{1 - \exp \left[- \int_z^{z_0} Ax^2 dx \int_0^{I(x)} f(I) dI \right]}{1 - \exp(-n_0 V)}$$

(1)

FOR OFFICIAL USE ONLY

FOR OFFICIAL USE ONLY

Utilizing the fact that the intensity of light in cross section z can be written in the form $I(z) = P_0/Az^2$, we rewrite equation (1) in the following manner:

$$P(z) = \frac{1 - \exp \left[-\frac{S_0^{3/2}}{2\sqrt{A}} \int_{S_0/Az^2}^{S_0/Az_0^2} \frac{dx}{x^{5/2}} \int_0^x \varphi(\xi) d\xi \right]}{1 - \exp(-n_0 V)}, \quad (2)$$

where $S_0 = P_0/I_0$; $\phi(\xi) = I_0 f(I_0 \xi)$; $\xi = I/I_0$; and I_0 is some typical value of intensity in the distribution $f(I)$, e.g., the mean or most probable. Let us now determine random magnitude z_i , equal to the distance from the focal point of the lens to the seat of failure at a maximum distance from it. We will assume that $z_i \gg \lambda_f$, where λ_f is the length of the lens's focal region. In this case the distribution density of magnitude z_i will be the function $W(z) = |dP(z)/dz|$, and the values of z and \bar{z}^2 can be found from the equations

$$\bar{z} = \int_0^{z_0} P(z) dz, \quad \bar{z}^2 = 2 \int_0^{z_0} z P(z) dz. \quad (3)$$

Equations (2) and (3) can be used to determine certain characteristics of distribution function $f(I)$.

Since in the case of $Vn_0 \gg 1$ the magnitude of z_i is determined by the behavior of $\phi(\xi)$ with low values of the argument, we will approximate it in this region by power functions. Let us consider two cases.

1. $\phi(\xi) = a\xi^k$. This approximation is based on the assumption of the existence of defects with low failure thresholds. Substituting it in (2) and with the tendency of $z_0 \rightarrow \infty$ we get the probability density:

$$W(z) = \frac{2k-1}{z_x} \left(\frac{z_x}{z}\right)^{2k} \exp \left[-\left(\frac{z_x}{z}\right)^{2k-1} \right], \quad (4)$$

$$z_x = \left[\frac{f^{(k)}(0) P_0^{k+1}}{k!(k+1)(2k-1)A^k} \right]^{1/(2k-1)}. \quad (5)$$

Let us note that distribution (4) represents the Weibull distribution [6] for the magnitude $1/z$ used for estimating the probability of electrical breakdown.

FOR OFFICIAL USE ONLY

FOR OFFICIAL USE ONLY

Employing (4), for the values of \bar{z} and \bar{z}^2 we get:

$$\bar{z} = \Gamma\left(\frac{2k-2}{2k-1}\right)z_x; \quad \bar{z}^2 = \Gamma\left(\frac{2k-3}{2k-1}\right)z_x^2, \tag{6}$$

where $\Gamma(x)$ is a gamma function and derivative $f^{(k)}(0)$ is related to coefficient a as follows:

$$a = I_0^{k+1} f^{(k)}(0) / k! .$$

For the root-mean-square fluctuation, $\overline{(z - \bar{z})^2}$, from (4) we have

$$\overline{(z - \bar{z})^2} = \gamma^2(k) \bar{z}^2 ,$$

where

$$\gamma(k) = \sqrt{\Gamma\left(\frac{2k-3}{2k-1}\right) - \Gamma^2\left(\frac{2k-2}{2k-1}\right)} / \Gamma\left(\frac{2k-2}{2k-1}\right).$$

With $k \gg 1$ we have $\gamma(k) \approx 1.28 / (2k - 1)$. Let us note that equations (6) can be used for an experimental estimate of parameter k .

For a more reliable determination of magnitudes k and $f^{(k)}(0)$ we will employ the method of maximum plausibility [8]. Let there be a sample $z_1 \dots z_n$ of capacity n with a random value of z_i . Having determined for it the logarithmic plausibility function

$$L = \sum_{i=1}^n \ln W(z_i, k, z_0) ,$$

we find the most effective estimates of parameters k and $f^{(k)}(0)$ from the system of equations

$$\frac{\partial L}{\partial z_x} = 0; \quad \frac{\partial L}{\partial k} = 0. \tag{7}$$

It can be easily solved numerically after transformation to the form

$$\frac{2n}{2k-1} - 2 \sum_{i=1}^n \ln z_i + 2n \frac{\sum_{i=1}^n (\ln z_i) / z_i^{1-2k}}{\sum_{i=1}^n 1 / z_i^{1-2k}} = 0; \tag{8}$$

FOR OFFICIAL USE ONLY

FOR OFFICIAL USE ONLY

$$z_k = \left(n \left/ \sum_{i=1}^n 1/z_i^{1-2k} \right. \right)^{1/2(k-1)}$$

Having found the root-mean-square deviations $S(k)$ and $S(f^{(k)}(0))$, of the most effective estimates of parameter k and $f^{(k)}(0)$ from the equation in [7],

$$S(x) = E[-\partial^2 L / \partial x^2]^{-1/2}$$

(E is the mathematical expectation arrived at by averaging in terms of the combined probability distribution), for k and $f^{(k)}(0)$ we get:

$$k = \hat{k} \pm \frac{\hat{k} - 1/2}{\sqrt{n}} \sqrt{\frac{2(\hat{k} - 1)}{4\hat{k} - 3}}; z_x = \hat{z}_x \pm \frac{\hat{z}_x}{(2\hat{k} - 1)\sqrt{n}}, \tag{9}$$

where \hat{k} and \hat{z}_x are solutions to system (8). Thus, equations (9) within the scope of a first approximation solve the problem posed of finding parameters of distribution $f(I)$ from the characteristics of sample z_1 .

2. $\phi(\xi) = a(\xi - 1)^k$. Here ξ is the intensity normalized for I_{\min} and I_{\min} is the minimum value of the threshold below which failure is impossible.

Making computations similar to sec 1 and estimating the integrals in (3) by the Laplace method, we get:

$$\bar{z} = (1 - \Delta) \sqrt{P_0 / (AI_{\min})}, \bar{z}^2 = (1 - 2\Delta) P_0 / (AI_{\min}) \tag{10}$$

$$\Delta = \frac{\Gamma(1/(k+2)) \left(\frac{k+2}{D} \right)^{1/(k+2)}}{2(k+2)}, D = \frac{a}{2(k+1)\sqrt{A}} \left(\frac{P_0}{I_{\min}} \right)^{3/2} \tag{11}$$

In deriving equation (10) it was assumed that $D \gg k + 2$. Equations (10) with high k can be used for approximate estimates of magnitudes I_{\min} and a . Employing the method of maximum plausibility, we find more precise values of parameters I_{\min} , a and k similarly to sec 1 from the system of the following equations:

$$\frac{\partial L}{\partial a} = \frac{n}{a} - \frac{z_{\max}^3 A}{2(k+1)(k+2)} \sum_{i=1}^n \left(\frac{z_{\max}^2}{z_i^2} - 1 \right)^{k+2} = 0;$$

FOR OFFICIAL USE ONLY

FOR OFFICIAL USE ONLY

$$\frac{\partial L}{\partial z_{\max}^2} = (k+1) \sum_{i=1}^n \frac{1}{z_i^2 (z_{\max}^2/z_i^2 - 1)} - \frac{3n}{2z_{\max}^2} - n(k+2) \frac{\sum_{i=1}^n \frac{1}{z_i^2} (z_{\max}^2/z_i^2 - 1)^{k+1}}{\sum_{i=1}^n (z_{\max}^2/z_i^2 - 1)^{k+2}} = 0;$$

$$\frac{\partial L}{\partial k} = \sum_{i=1}^n \ln \left(\frac{z_{\max}^2}{z_i^2} - 1 \right) + \frac{n}{k+2} - n \frac{\sum_{i=1}^n (z_{\max}^2/z_i^2 - 1)^{k+2} \ln (z_{\max}^2/z_i^2 - 1)}{\sum_{i=1}^n (z_{\max}^2/z_i^2 - 1)^{k+2}} = 0;$$

(12)

where $z_{\max}^2 = P_6 / AI_{\min}$.

4. Discussion of Results Obtained

Let us discuss the applicability of the method described above for determining the parameters of distribution $f(I)$ from characteristics of a sample of random magnitude z_i . Let us note that fluctuations in the distance to the last fracture, z_i , generally speaking, can be caused for two reasons: the finiteness of the total number of particles in the space considered, and the variance in the failure threshold in different defects. Of course, the parameters of function $f(I)$ can be found from magnitude z_i only in the second case. Actually if $f(I) = \delta(I - I_p)$, fluctuations in z_i will be caused only by the finiteness of the concentration of defects--

$$(\overline{\Delta z^2})^{1/2} = I_p / n_0 p_0.$$

Consequently, the problem of finding the parameters of $f(I)$ can be solved if the characteristic breadth, ΔI , of function $f(I)$ satisfies the inequality

FOR OFFICIAL USE ONLY

FOR OFFICIAL USE ONLY

$$\frac{dI}{dz} \sqrt{\Delta z^2} = \frac{2A^{1/2} I_n^{5/2}}{n_0 P_0^{3/2}} \ll \Delta I.$$

It is obvious that this fulfillment can be achieved by increasing P_0 up to values representing a changeover from the equation $(\Delta z^2)^{1/2} \approx 1/P_0$ to the relationship defined by equation (10).

Let us note that for sufficiently narrow distributions of $f(I)$ this changeover can occur with high values of P_0 such that fluctuations Δz^2 become quite slight. The triviality of Δz^2 places requirements on the permissible amount of the relative fluctuation in the power of the laser emission: $\Delta P_0/P_0 \ll [(2k-1)/(k+2)]\gamma(k)$ (cf. equation (6)) for a first approximation, or $\Delta P_0/P_0 \ll \Delta$ (cf. equation (11)) for a second approximation. Earlier we considered as an example two approximations of $f(I)$. The question of the applicability of a specific approximation of $f(I)$ for a given specific substance can be solved by means of statistical methods of verifying hypotheses, e.g., from the dependence of z and z^2 on P_0 . The equations obtained above can be used for analyzing the form of function $f(I)$ if the mechanism of the defect's failure is strongly nonlinear and can be characterized by the value of the threshold intensity. This can take place, for example, in the thermal rupture of absorbing defects [8], with an electronic avalanche and in multi-photon ionization.

5. Experiment

The technique suggested was employed by us for the purpose of determining parameters of the distribution function of microdefects from failure thresholds in silicon and gallium arsenide. An investigation was made of single crystals of high-resistance dislocation-free silicon containing defects of the B-cluster type, and of semi-insulating gallium arsenide [2].

The radiation of a pulsed supermode CO_2 laser ($\tau_i = 10^{-7}$ s) was focused inside the sample by a silicon contact lens [5]. The geometry of the focusing system made possible practically uniform distribution of intensity over the cross section of the beam, with $A = 0.12$. The power of the radiation, P_0 , in the Si crystal equaled approximately 60 kW, and in the GaAs, approximately 15 kW, which was approximately an order of magnitude higher than the threshold value. The fracture took the form of a cone, consisting of individual foci (fig 2 [photograph not reproduced]). As magnitude z_1 was used the distance between the threshold fracture located on the lens's caustic and the fracture most remote from it. Statistical processing of the experimental results was performed on the basis of the first approximation. Relative fluctuations of $\Delta P_0/P_0$ were determined by the stability of pumping and equaled approximately two percent. The selection of the first approximation equation for an approximation of $f(I)$ in the region of low intensities was justified by the fact of an

FOR OFFICIAL USE ONLY

FOR OFFICIAL USE ONLY

increase in the magnitude of Δz^{-2} with an increase in P_0 (cf. equation (6)).

The results arrived at, averaged for 20 realizations, are given in the table.

Table

1) Материал	\bar{z} , см	2) $\sqrt{\Delta z^2}$, мкм.	k	3) $f^k(0)$, $(\text{см}^2/\text{МВт})^{k+1} \cdot \text{см}^{-3}$	4) I_p , $\text{ГВт}/\text{см}^2$
Si, 1	$127,6 \cdot 10^{-4}$	14,7	8 ± 1	$(5,5 \pm 1,2) \cdot 10^{-10}$	3
Si, 2	$135,4 \cdot 10^{-4}$	23,1	5 ± 1	$(2,9 \pm 0,6) \cdot 10^{-8}$	2,6
GaAs	$191,1 \cdot 10^{-4}$	24,5	6 ± 1	$(4,5 \pm 1) \cdot 10^{-8}$	0,35

Key:

1. Material
2. Microns

3. $\text{см}^2/\text{МВт}$
4. $\text{ГВт}/\text{см}^2$

The values of \bar{z} and $(\Delta z^2)^{1/2}$ in the table were obtained from equations (6) and of $f^k(0)$ and k from equations (8); I_p is the threshold intensity of failure with the area of the laser beam's cross section, Δz^2 . Let us note that the proximity of the failure threshold on the lens's caustic, I_p , to the magnitude of I_0 , as well as the high value of parameter k , indicate the short breadth of distribution function $f(I)$. Furthermore, attention is drawn by the slower growth in $f(I)$ with low intensities in silicon sample No 2, obtained with lower rates of growth.

6. Conclusion

The theory developed above for the statistics of laser failure in micro-defects demonstrates that when employing focused radiation fluctuations in the appearance of the seat of damage most remote from the focal point are determined by low-threshold defects. This has made it possible to suggest a new procedure for determining the parameters of the distribution function of defects from failure thresholds in the region of low intensities. Although in the analysis presented we were restricted to two kinds of approximation of distribution function $f(I)$, it is obvious that a similar discussion can be given for other approximations also.

Experiments conducted with monocrystalline silicon have demonstrated that the procedure suggested is quite sensitive to changes in the parameters of defects in crystals caused, for example, by different rates of growth.

FOR OFFICIAL USE ONLY

FOR OFFICIAL USE ONLY

This points toward the possibility of using it as a new method of explaining mechanisms for the formation and diagnosis of impurity-type microdefects of submicron size which are difficult to detect by other methods.

It should be mentioned that the form of function $f(I)$ depends not only on the parameters of defects, but also on the characteristics of the laser radiation (pulse length and wavelength). The revelation of this dependence can provide additional information on the mechanism of laser failure.

The authors wish to thank F.V. Bunkin and A.A. Manenkov for their interest in this study and helpful discussions.

Bibliography

1. Danileyko, Yu.K., Manenkov, A.A., Nechitaylo, V.S. and Ritus, A.I. KVANTOVAYA ELEKTRONIKA, 1, 1812 (1974).
2. Petroff, P.M. and de Kock, A.J.R. J. CRYST. GROWTH, 30, 17 (1975).
3. Aleshin, N.A., Anisimov, S.I., Bonch-Bruyevich, A.M., Imas, Ya.I. and Komolov, V.L. ZHETF, 70, 1214 (1976).
4. Danileyko, Yu.K., Lebedeva, T.P., Manenkov, A.A. and Sidorin, A.V. ZHETF, 74, 765 (1978).
5. Bunkin, F.V. and Savranskiy, V.V. ZHETF, 65, 2185 (1973).
6. Fischer, P.H.H. and Nissen, K.W. IEEE TRANS., EL-11, 37 (1976).
7. Khudson, D. "Statistika dlya fizikov" [Statistics for Physicists], Moscow, Mir, 1967.
8. Danileyko, Yu.K., Manenkov, A.A., Nechitaylo, V.S., Prokhorov, A.M. and Khaimov-Mal'kov, V.Ya. ZHETF, 63, 1030 (1972).

COPYRIGHT: Izdatel'stvo Sovetskoye Radio, KVANTOVAYA ELEKTRONIKA, 1979 [83-8831]

CSO: 1862
8831

FOR OFFICIAL USE ONLY

FOR OFFICIAL USE ONLY

UDC 621.378.9

INVESTIGATION OF LIMITING OPERATING MODES OF A LAMP-TYPE PUMPING MODULE
IN THE 'MIKRON' LASER UNIT

Moscow KVANTOVAYA ELEKTRONIKA in Russian Vol 6 No 12, 1979 pp 2606-2609
manuscript received 7 May 79

[Article by B.V. Yershov, V.A. Spiridonov and V.B. Fedorov, USSR Academy
of Sciences Physics Institute imeni P.N. Lebedev, Moscow]

[Text] In the pumping pulse length range of 0.1 to 3 ms a determination
is made of the maximum power of xenon lamps used for pumping large-scale
neodymium-doped glasses. A study is made of the influence of the design
of a Kh-122-PM light source on the maximum power of pumping lamps. The
operating life, estimated from the data obtained, of a multi-lamp module
agrees with the experience gained in using the "Mikron" unit.

The "Mikron" unit [1] is a high-power neodymium laser created on the basis
of large-scale active elements with a rectangular cross section measuring
72 X 24 X 4 cm and a light source of the Kh-122-PM type. The active ele-
ments are pumped by means of lamp modules, each of which is in the form of
a bank of 18 lamps (fig 1). In terms of circuitry, a module consists of
nine discharge circuits with two series-connected lamps in a circuit, with
each circuit powered from independent sections of a capacitor bank. De-
signwise, the discharge circuits are so assembled that currents in lamps
placed in a row are aimed in opposite directions. The entire pumping sys-
tem of the "Mikron" unit contains 36 of these unified modules.

For the purpose of ensuring a reliable operating mode for a multi-lamp
pumping module it is necessary to investigate its limiting load character-
istics. This problem is of general importance, since the pumping systems
of all high-power solid state lasers are of the multi-lamp type.

The operating life of a multi-lamp module is determined primarily by the
operating life of a single lamp, N , which is described by the following
empirical equation [2]:

$$N = (W_{np}/W)^{0.8},$$

FOR OFFICIAL USE ONLY

FOR OFFICIAL USE ONLY

where N is the maximum possible number of flashes with energy of W and W_{pr} is the maximum load on a lamp causing it to go out of order with the first flash. In multi-lamp pumping systems W_{pr} , and this means the life-time, N , too, are reduced as a function of the design of the light source [3-5]. Since W is usually predetermined by the requirements for the level of population inversion of the working transition in the active medium (in our case $W \approx 5$ kJ for a single lamp with a pulse length of $\tau \approx 0.35$ ms at the level of 0.35 times the peak value), then the magnitude determining the operating life of a multi-lamp pumping module equals W_{pr} .

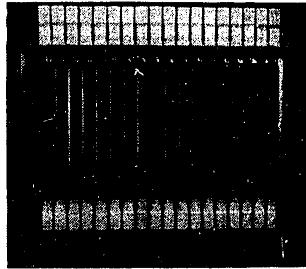


Figure 1. Multi-Lamp Pumping Module (Based on Kh-122-PM Unit) of the "Mikron" Unit

In this study were investigated three types of lamps (fig 2) used in the Kh-122-PM light source. Their key parameters are given in the table. From the data in [6] on the value of W_{pr} for a single IFP-8000 lamp operating in the mode indicated above, the operating life is about 100 flashes; taking into account the reduction in W_{pr} as the result of the influence of the light source [3], the number of flashes becomes on the order of 10, which is obviously inadequate for the operation of a multi-lamp pumping system. For the other two types of lamps (IFP-8000-1 and INP-18/250) there are no data on the $W_{pr}(\tau)$ dependence in the pulse length range of interest to us, of $0.1 \text{ ms} < \tau < 1 \text{ ms}$ (an analog of the IFP-8000-1 lamp was investigated earlier in [8], but with $\tau \approx 0.01 \text{ ms}$). Therefore the first goal of our study has been to determine the dependence $W_{pr}(\tau)$ for IFP-8000-1 and INP-18/250 lamps.

FOR OFFICIAL USE ONLY

FOR OFFICIAL USE ONLY

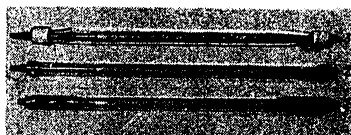


Figure 2. Types of Lamps Used in the Kh-122-PM Light Source: the IFP-8000 with a Foil Current Lead (1) and the IFP-8000-1 with a Cap-Type Current Lead (2) and the INP-18/250 (3)

Table

Type of lamp	Distance between electrodes, cm	Inside diameter, cm	Wall thickness, mm	Type of lead-in	Pressure, mm Hg	V_k/V_0^*
IFP-8000	25	1.6	1.3-1.6	Foil	300	0.1
IFP-8000-1	25	1.6	1.2-1.8	Cap	300	0.35
INP-18/250	25	1.8	2.0-2.5	Cap	300	0.27

* V_k/V_0 is the ratio of the space beyond the electrodes to the total inside space of the lamp.

The procedure for determining the maximum power is similar to that given in [7] with a number of flashes in a series of not less than three. The pulse length and power, W , were changed by altering the voltage, inductance and capacitance of the discharge circuit. Curves obtained for $W_{pr}(\tau)$ are given in fig 3. The $W_{pr}(\tau)$ curve for the IFP-8000 lamp is taken from [6] and the data of our pr experiments on this lamp agree with this.

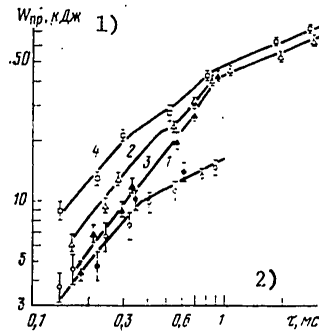
The $W_{pr}(\tau)$ curve reveals, as in the experiments in [6], a change in the slope of the time dependence of maximum power with $0.3 \text{ ms} < \tau < 0.7 \text{ ms}$. In the region of long pulses of $\tau > 0.7 \text{ ms}$ the dependence of the maximum power on the pulse length equals $W_{pr} \sim \tau^{1/2}$, i.e., is slighter than the

FOR OFFICIAL USE ONLY

FOR OFFICIAL USE ONLY

dependence of $W_{DP} \sim \tau$ in the region of short pulses of $\tau < 0.3$ ms. From a comparison of the curves in fig 3 it is obvious that for lamps with a greater wall thickness the values obtained for the maximum power are higher, and this increase is most significant in the region of short pulses ($\tau < 0.3$ ms). In the region of long pulses ($\tau > 0.8$ ms) the maximum power for IFP-8000-1 and INP-18/250 lamps differ insignificantly. The strong difference in the maximum power for IFP-8000 and IFP-8000-1 lamps is explained evidently by the difference in design and fabrication technology.

For the purpose of determining the reliability of operation of the entire pumping system as a whole it is necessary to determine to what extent W_{DP} is lowered when going from a single lamp in free space to a multi-lamp system placed in a light source. One of the chief reasons for the reduction in W_{DP} in a light source is thought to be the increase in the amplitude of the current flowing through a lamp as the result of the absorption of the radiation of neighboring lamps and the radiation returned from reflectors [3-5]. Experiments conducted have demonstrated that in our case the current in a lamp, within the limits of measurement accuracy of 15 percent, is identical both for a single lamp and when the same lamp is operating in a group of 18 lamps placed in a Kh-122-PM light source. As a reflector was used aluminum foil with reflectance of $r \sim 0.6$. Measurements of maximum power make it possible to assert that W_{DP} in this design of a light source practically does not depend on whether one or 18 lamps is working in the light source. As a result of these experiments it was found that the factor influencing W_{DP} in a light source is the existence of a closely placed wall (at a distance of 1.2 cm from the surface of the lamp). In fig 3 is shown the $W_{DP}(\tau)$ curve with the presence of a closely placed wall for the IFP-8000-1 lamp (curve 2a). It is obvious from comparing curves 2 and 3 that the most substantial reduction in W_{DP} takes place with short pulses ($\tau < 0.3$ ms); this reduction practically disappears with $\tau \sim 0.8$ ms.



[Caption and key on following page]

FOR OFFICIAL USE ONLY

FOR OFFICIAL USE ONLY

Figure 3. Dependences of Maximum Loads on Pulse Length for an IFP-8000 Lamp (1) from the Data in [6] (White Dots) and from the Data of Our Study (Black Dots), for an IFP-8000-1 Lamp in Free Space (2) and Near the Wall of the Light Source (3), and for an INP-18/250 Lamp in Free Space (4)

Key:

1. W_{pr} , kJ

2. τ , ms

By utilizing curve 2, it is possible to estimate the operating lifetime of a pumping system in this mode ($\tau \sim 0.35$ ms and $W = 5$ kJ)—approximately 800 flashes. The data on the operation of a pumping system arrived at over the course of two years of operation give a value of about 200 flashes, which in order of magnitude agrees with the estimate given. For INP-18/250 lamps this estimate according to the data in fig 3 gives about 10^4 flashes. As the result of using an individual Kh-122-PM light source with two pumping modules (36 lamps of the INP-18/250 type), after 200 flashes in the working mode no change was detected in the parameters of the lamp, which does not contradict the estimate given.

The data obtained make it possible to speak of the high reliability of the pumping system of the "Mikron" unit and indicate the promise of developing multi-lamp pumping systems for high-power solid state lasers.

Bibliography

1. Batanov, V.A., Bogatyrev, V.A., Bufetov, I.A., Gusev, S.B., Yershov, B.V., Kolisnichenko, P.I., Malkov, A.N., Prokhorov, A.M., Spiridonov, V.A., Fedorov, V.B. and Fomin, V.K. *IZV. AN SSSR, SER. FIZICHESKAYA*, 42, 2504 (1978).
2. Waszak, L. *MICROWAVES*, 8, No 5, 132 (1969).
3. Mak, A.A. and Shcherbakov, A.A. *KVANTOVAYA ELEKTRONIKA*, No 5 (17), 68 (1973).
4. Basov, Yu.G., Ivanov, V.V., Makarov, V.N., Narkhova, G.I. and Shcherbakov, A.A. *OPTIKA I SPEKTROSKOPIYA*, 38, 608 (1975).
5. Kirsanov, V.P., Troshkin, S.V. and Bykov, I.V. *KVANTOVAYA ELEKTRONIKA*, 3, 431 (1976).
6. Kirsanov, V.P., Troshkin, S.V. and Bykov, I.V. *KVANTOVAYA ELEKTRONIKA*, 2, 181 (1975).
7. Marshak, I.S., editor. "Impul'snyye istochniki sveta" [Pulsed Light Sources], Moscow, Energiya, 1978.

FOR OFFICIAL USE ONLY

FOR OFFICIAL USE ONLY

8. Podgayetskiy, V.N. and Skvortsov, B.N. KVANTOVAYA ELEKTRONIKA,
No 4 (10), 82 (1972).

COPYRIGHT: Izdatel'stvo Sovetskoye Radio, KVANTOVAYA ELEKTRONIKA, 1979
[83-8831]

CSO: 1862
8831

FOR OFFICIAL USE ONLY

FOR OFFICIAL USE ONLY

UDC 621.383.8

INVESTIGATION OF CHARACTERISTICS OF NEW COMPOSITIONS FOR PASSIVE SHUTTERS FOR IODINE LASERS

Moscow KVANTOVAYA ELEKTRONIKA in Russian Vol 6 No 12, 1979 pp 2652-2653
manuscript received 12 Jul 79

[Article by S.P. Batashev, M.G. Gal'pern, V.A. Katulin, O.L. Lebedev, Ye.A. Luk'yanets, N.G. Mekhryakova, V.M. Mizin, V.Yu. Nosach, A.L. Petrov and V.A. Petukhov, USSR Academy of Sciences Physics Institute imeni P.N. Lebedev, Moscow]

[Text] A report is given on the creation of two dye compositions which clear under the influence of the radiation of an iodine laser ($\lambda = 1.315 \mu$) and have low residual absorption.

For the purpose of eliminating self-excitation in high-power iodine laser units, as optical decouplers between amplifier stages are used clearing filters based on atomic iodine [1] and solutions of organic dyes [2]. Filters based on iodine are complicated to use, since in working with them it is necessary to maintain the temperature of the cell at about 800°C. Clearing filters based on solutions of organic dyes are simpler and more reliable and can be used in laser beams with practically any aperture.

An important parameter of clearing compositions influencing the output power of a laser unit is the amount of residual absorption in the cleared state; therefore the creation of clearing compositions with reduced residual absorption is a topical problem.

In this study a report is given on the creation of new compositions based on dyes 1061 and 1067 which clear under the effect of the radiation of a photodissociation iodine laser with a wavelength of 1.315 μ , and the results are given of an investigation of their key characteristics. Measurements of the parameters of solutions of dyes were made with an iodine laser with a power of approximately 3 J and a pulse length of approximately 1 ns. The transmittance of the compositions in determining its dependence on the power density of the incident radiation was determined as the ratio of the power of the laser pulse having passed through the cell with the composition and of that hitting the cell. The power density of the radiation hitting

FOR OFFICIAL USE ONLY

FOR OFFICIAL USE ONLY

the cell (beam diameter of 1 cm) was varied by means of neutral filters and the pulse energy before and after the cell was measured by calorimeters.

In fig 1 are given curves for the transmittance of solutions of dyes 1061, 1067 and 1057 (a report was given on the latter in [2]), having different initial transmittance. From a comparison of these curves it is obvious that compositions 1061 and 1067 have lower residual losses than the solution of dye 1057 developed earlier.

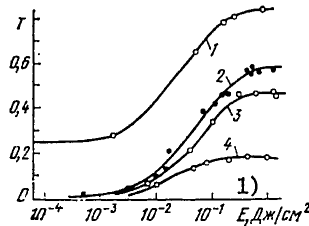


Figure 1. Dependence of Transmittance, T , of Investigated Compositions with Different Initial Transmittance on Power Density of Incident Radiation: 1--1067, $T_0 = 0.25$; 2--1067, $T_0 = 0.004$; 3--1061, $T_0 = 0.006$; 4--1057, $T_0 = 0.01$

Key:
1. J/cm^2

We also studied Sulfolan solutions of dyes No 1, 2 and 3, close in structure to dye BDN II in which good clearing was achieved in [3]. The best clearing was arrived at with dye No 3, whose absorption spectrum is identical to the spectrum given in [3] for BDN II in Sulfolan, but it is much worse than with dyes 1061 and 1067. In the table, for all the dyes studied, are given ratios of the original optical density, D_0 , to the optical density in the cleared state, D_{pr} , found from the clearing curve.

Table

1) Краситель	2) Начальное пропускание	3) D_0/D_{pr}	Краситель	Начальное пропускание	D_0/D_{pr}
№ 1	0,16	$1,2 \pm 0,1$	1061	0,085	$6,9 \pm 0,7$
№ 2	0,14	$1,4 \pm 0,2$	1061	0,006	$6,8 \pm 0,7$
№ 3	0,41	$2,8 \pm 0,2$	1067	0,25	$7,7 \pm 1,0$
1057	0,12	$4,2 \pm 0,5$	1067	0,004	$9,2 \pm 1,5$

[Key on following page]

FOR OFFICIAL USE ONLY

FOR OFFICIAL USE ONLY

Key:

1. Dye
2. Original transmittance
3. D_0/D_{pr}

Another important characteristic of a clearing composition is the time for relaxation of the cleared state. For the purpose of determining the relaxation time of a composition was employed a system with a variable optical delay line (OLZ). Part of the radiation of the iodine laser cleared the cell with the solution and another part of the radiation, after the OLZ, was reduced by neutral filters and also passed through the cell. By measuring the energy of the delayed pulse before and after the cell, we determined the transmittance of the cell at different moments of time after the clearing pulse passed through. The relaxation time for the cleared state of solutions of dyes 1057, 1061 and 1067 determined from these measurements equaled 20 ± 10 ns.

By means of the compositions developed, passive Q switching of an iodine laser was accomplished. The laser's cavity was formed by flat mirrors with reflection coefficients of 100 and eight percent and the distance between them varied from 110 to 220 cm. The design and parameters of the laser head and the composition of the working mixture were the same as in [2]. By selection of the key parameters of the laser and by employing as a passive shutter a cell with a solution of a dye having an original transmittance of $T_0 = 10$ percent was achieved the generation of a single giant pulse. With a cavity length of 110 cm the pulse had a smooth shape with a duration of 20 ns, and with an increase in the length there appeared amplitude modulation, reaching 100 percent with a cavity length of 220 cm (fig 2). The shape of the pulse was recorded by a high-speed I2-7 oscillograph connected to a coaxial FEK-31KP photocell. In the case of 100-percent modulation, the laser's radiation represented a chain of individual peaks, as is usually observed in lasers with self-synchronization of modes. The length of an individual peak was 4 ns. Such a long length of an individual peak as compared with the ultrashort pulses of solid state lasers with self-synchronization of modes is explained by the narrow breadth of the lasing spectrum of an iodine laser, which is approximately 0.01 cm^{-1} at the pressures employed for the gas mixtures. In this case with a cavity length of 220 cm the number of lasing modes is not greater than three or four. The length of an individual peak cannot be shorter than t_0/m , where t_0 is the time for double passage through the cavity (in our case $t_0 = 15$ ns) and m is the number of excited modes; consequently, the length of a peak with self-synchronization of this number of modes should equal 3 to 4 ns, which has been observed experimentally.

The compositions developed by us, in addition to low residual absorption, have high resistance to the influence of laser radiation and do not change their properties during longterm storage, which makes them promising for employment in iodine laser systems.

Employment of passive shutters based on dyes 1061 and 1067 in a high-power iodine laser unit at the USSR Academy of Sciences Physics Institute has

FOR OFFICIAL USE ONLY

FOR OFFICIAL USE ONLY

made it possible substantially to improve emission parameters. With a radiated power of about 100 J a contrast of 10^8 was achieved [4].

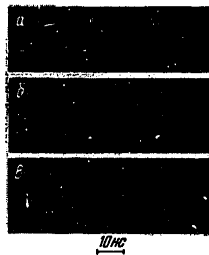


Figure 2. Oscillograms of Lasing Pulses of an Iodine Laser with Passive Q Modulation by Means of a Dye Solution ($T_0 = 0.10$) with a Cavity Length of 110 (a), 145 (b) and 220 cm (c)

Key:

1. 10 ns

In conclusion the authors wish to thank V.N. Koprashenkov for his helpful discussions and for offering analogs of BDN II.

Bibliography

1. Gaydash, V.A., Yeroshenko, V.A., Lapin, S.G., Shemyakin, V.I. and Shurygin, V.K. KVANTOVAYA ELEKTRONIKA, 3, 1701 (1976).
2. Gal'pern, M.G., Gorbachev, V.A., Katulin, V.A., Lebedev, O.L., Luk'yanets, Ye.A., Mekhryakova, N.G., Mizin, V.M., Nosach, V.Yu., Petrov, A.L. and Semenovskaya, G.G. KVANTOVAYA ELEKTRONIKA, 2, 2531 (1975).
3. Beaupere, D. and Farcy, J.C. OPTICS COMM., 27, 410 (1978).
4. Basov, N.G., Zuyev, V.S., Katulin, V.A., Lyubchenko, A.Yu., Nosach, V.Yu. and Petrov, A.L. KVANTOVAYA ELEKTRONIKA, 6, 311 (1979).

COPYRIGHT: Izdatel'stvo Sovetskoye Radio, KVANTOVAYA ELEKTRONIKA, 1979 [83-8831]

CSO: 1862
8831

END

51

FOR OFFICIAL USE ONLY